Journal of Hydrology 498 (2013) 319–334

Contents lists available at SciVerse ScienceDirect

Journal of Hydrology

journal homepage: www.elsevier.com/locate/jhydrol

Pathways and processes associated with the transport of groundwater in deltaic systems

Alexander S. Kolker [a,c,*], Jaye E. Cable [b], Karen H. Johannesson [c], Mead A. Allison [d], Lorna V. Inniss [e]

[a] Louisiana Universities Marine Consortium, 8124 Highway 56, Chauvin, LA 70344, United States
[b] Department of Marine Sciences, University of North Carolina-Chapel Hill, Chapel Hill, NC 27599, United States
[c] Department of Earth and Environmental Sciences, Tulane University, New Orleans, LA 70118, United States
[d] Water Institute of the Gulf, Baton Rouge, LA, United States
[e] Coastal Zone Management Unit, Bay Street, St. Michael, Barbados

ARTICLE INFO

Article history:
Received 16 February 2013
Received in revised form 10 May 2013
Accepted 8 June 2013
Available online 20 June 2013
This manuscript was handled by Corrado Corradini, Editor-in-Chief, with the assistance of Diana M. Allen, Associate Editor

Keywords:
Submarine groundwater discharge
Mississippi River Delta
Paleochannel

SUMMARY

Rivers are considered to be the primary means driving hydrological and geochemical fluxes between the continents and the ocean. However, it is unclear how well surface water fluxes represent total fluxes, or whether more diffuse subterranean fluxes of river water to the coastal ocean occur. This question is important in light of research demonstrating that submarine groundwater discharge (SGD) is important for geochemical and hydrological fluxes. Here, we examine the pathways and potential magnitude of the role that SGD plays in the Mississippi River Delta (MRD), the largest delta in North America. We present multiple independent lines of evidence demonstrating a hydrological connection between the Mississippi River (MR) and the MRD. Evidence includes hydrological budgets demonstrating downstream water losses from the MR, which are unexplained and are of the same magnitude as water sources to adjacent coastal bays of the MRD; well data indicating a correlation between groundwater height and the stage of the MR; and excess ^{222}Rn inventories exceeding that expected from in situ production, implying an advective, i.e., groundwater source, to coastal bays. SGD likely flows from the MR to its delta via paleochannels and other buried sand bodies. Seismic data indicates that such features are common, whereas resistivity data suggest the intrusion of low salinity water to coastal bays adjacent to the river. These results may be applicable to other deltas worldwide, as many of the world largest rivers have deltas with numerous abandoned distributaries that could act as conduits for groundwater.

1. Introduction

Rivers are generally considered to be the primary means by which material is transferred from the continents to the oceans (McKee et al., 2004; Meybeck, 1982; Milliman and Meade, 1983). Global geochemical budgets indicate that rivers are responsible for almost 100% of the 308×10^{12} g of Cl^-, 76% of the 236×10^{12} g of Si, and 76–80% of the $102–123 \times 10^{12}$ g of N that are presently delivered to the world's oceans (Berner and Berner, 1996). Even after decades of research, many questions remain about the magnitude and timing of many of these fluxes (McKee et al., 2004). Some of these questions reflect the fact that most hydrological and geochemical measurements are obtained upstream of the region of tidal influence, which can be 100s of km inland, and thus do not adequately account for impacts of estuarine processes such as particle aggregation and microbial respiration on geochemical fluxes (McKee et al., 2004), or effects of lowland floodplain/delta plain sources and sinks (Bianchi and Allison, 2009). However, other important questions also remain: how well do the fluxes of dissolved constituents in rivers reflect the total flux of water and elements to the ocean, and does a more diffuse and lower velocity, subterranean, river stage-driven groundwater flux to the coastal ocean exist?

Over the past two decades substantial effort has occurred in the scientific community to quantify the submarine flux of groundwater to the oceans (e.g., Burnett et al., 2006; Cable et al., 1996b; Charette et al., 2003; Moore, 2010; Rama and Moore, 1996). Termed *submarine groundwater discharge* (SGD), a majority of the estimates of the global, terrestrial-derived flux of SGD range between 5% and 10% of the annual global river water discharge to the ocean (Burnett et al., 2006, 2003, 2001; Moore, 1999, 2010; Zekster and Loaiciga, 1993). Many of these studies also indicate that the geochemical significance of SGD fluxes is far greater than would be expected from volumetric considerations alone, as groundwaters are commonly enriched in nutrients, contaminants, metals, and radioisotopes. For example, SGD is shown to be an

* Corresponding author. Address: Louisiana Universities Marine Consortium, 8124 Highway 56, Chauvin, LA 70344 USA. Tel.: +1 504 579 2427.
E-mail addresses: akolker@lumcon.edu (A.S. Kolker), jecable@email.unc.edu (J.E. Cable), kjohanne@tulane.edu (K.H. Johannesson), mallison@thewaterinstitute.org (M.A. Allison), linniss@coastal.gov.bb (L.V. Inniss).

0022-1694/$ - see front matter © 2013 Elsevier B.V. All rights reserved.
http://dx.doi.org/10.1016/j.jhydrol.2013.06.014

important source of nitrogen to Massachusetts estuaries (Kroeger and Charette, 2007; Valiela and Teal, 1979), Fe to the southern ocean (Windom et al., 2006), and rare earth elements to coastal waters (Johannesson et al., 2011). Despite these advances, many of the most detailed studies of SGD have focused on small sandy aquifers or broad karstic settings (Charette et al., 2005, 2003; Dulaiova et al., 2006a), rather than major river deltas (Burnett et al., 2006; Moore, 2010; Taniguchi et al., 2002). Whereas deltas make up only a small fraction of Earth's coastlines, their geological and geochemical significance is tremendous. Deltas are major sediment depocenters (Roberts, 1997), highly productive ecologically, feature a diversity of sediment types, are sites of authigenic mineral formation (Lowers et al., 2007; Michalopoulos and Aller, 1995), and serve as a primary locus for the burial, remineralization, and export of nutrients and carbon (Aller and Blair, 2004; Bianchi and Allison, 2009; Bianchi et al., 2011b; Burdige, 2005). As such, it is reasonable to expect that major river deltas are important sources of SGD to the coastal ocean. Indeed, the few studies that have examined SGD in large river deltas have found groundwater plays an important role in hydrological and geochemical fluxes (Basu et al., 2001, 2002; Dulaiova et al., 2006b; Georg et al., 2009; Harvey, 2002; Kim et al., 2005; Krest et al., 1999; Moore and Krest, 2004; Peterson et al., 2008). For example, groundwater in the Ganges–Brahamaputra Delta is an important source of both Si and Sr to the global ocean (Basu et al., 2001; Georg et al., 2009), whereas SGD in the Yellow River Delta in China is an important source of Si to the Bohai Sea (Kim et al., 2005).

Here we explore the potential role of deltas as a pathway for SGD by examining the hypothesis that there is appreciable discharge by this pathway to the Mississippi River Delta (MRD), the archetype of a river-dominated delta (Coleman et al., 1998). We show that SGD fluxes are potentially large enough to alter surface water budgets and the salinity distribution of coastal bays in the MRD system. Further, we hypothesize that SGD fluxes in the MRD are likely to vary both spatially and temporally, with highest fluxes occurring during high discharge events, and along buried deposits of course-grained material. Our results demonstrate a mechanism for delivering groundwater in deltaic systems, which are notorious for their anisotropic and heterogeneous depositional patterns; and when combined with other studies in the literature, suggest that deltas worldwide may be an important source of SGD to the world's oceans.

2. Setting

The MRD is one of the largest deltas on Earth, and is the largest such system in North America (Fig. 1). The Mississippi River (MR) is the sixth largest river globally in terms of discharge, the seventh largest in terms of suspended sediment load, and the world's third largest river system in terms of drainage area (McKee et al., 2004; Milliman, 1991). The MR is also the largest source of freshwater, sediment, and nutrients to the Gulf of Mexico (Dunn, 1996), delivering an average of 534×10^9 m^3 of freshwater, 88.3×10^6 tons of sediment, and 4.0×10^{12} moles of organic carbon to the Gulf of Mexico annually (Allison et al., 2012; Bianchi et al., 2004; Solis and Powell, 1999). The MRD formed over the past 7000 years, after the stabilization of Holocene sea-level, as a series of avulsions changed the outlet of the river, which deposited sediments across several hundred kilometers of what is now the Louisiana coastline (Roberts, 1997). Each avulsion formed a new delta lobe, building an area of several thousand km^2, and the periods between avulsions typically ranged between 700 and 1400 years (Roberts, 1997; Törnqvist et al., 1996). As individual delta lobes aged, distributary channels were abandoned and received a decreasing quantity of river flow (Roberts, 1997). These abandoned river channels were typically sandy beds, which formed either slow-moving bodies of water locally known as bayous, or were subsequently buried forming paleochannels (Coleman and Prior, 1980; Roberts, 1997). As bayous aged and filled in with organic material and fine-grained sediments, the buried sand deposits of their banks and bottoms became available as conduits for river water to enter the coastal ocean through subterranean flow paths. Sand deposits in the MRD are also associated with barrier island chains, which are typically river sediments reworked by waves and tides (Coleman and Prior, 1980). Between these old river channels a network of interdistributary bays developed. Examples of these bays include Barataria and Terrebonne Bays located south and west of the Mississippi River (Fig. 1), each with vast expanses of coastal wetlands. Furthermore, the Mississippi River is flanked by numerous crevasse splays, which formed during the 19th and early 20th centuries (Day et al., 2012; Roberts, 1997). These splays are commonly sand-rich (Esposito et al., 2013; Roberts, 1997), and also have the potential to serve as conduits for groundwater flow.

The present-day course of the main stem Mississippi River passes New Orleans on its way to the Gulf of Mexico (Fig. 1). However, at 506 river kilometers (RK506) upriver of the Head of Passes (the Bird's Foot mouth), the flow of the Mississippi River is diverted by the Old River Control Structure into the Atchafalaya Basin, where it mixes with waters from the Red River to form the Atchafalaya River. As such, the daily flow down the Atchafalaya reach is controlled at 30% of the combined flow of the Mississippi and Red Rivers. The Mississippi River pathway above and below Old River is relatively constrained by levees faced with concrete mats in shallow water from several 1000 km inland to near the RK 18 on the west bank of the river and RK 72 on the river's east bank. Below Baton Rouge, LA, (RK 372) these levees constrain the river to within 1 km of the channel (Allison et al., 2012). These levees limit or restrict lateral channel migration, crevassing and overbank flow, and function to increase stage during high discharge events. Whereas both natural and artificial levees appear along the Atchafalaya River (below Old River), these levees constrain the flow of this river to within 5 km of its main channel in the upper reaches, and leave much greater room to migrate laterally in its lower reaches (Allison et al., 2012). These structures reduce the magnitude of stage maximums, particularly in the lower Atchafalaya River, during high discharge events.

3. Methods and data sources

Data used in the present study come from several different sources all of which can be used to track the flow of water from the Mississippi River into coastal bays in the MRD. This study will focus on Barataria Bay (Fig. 1), a 4100 km^2 interdistribuary bay, with a basin that covers about 20% of the MRD (Reed et al., 1995). Bararatia Bay has a similar tidal regime (~30-cm diurnal tide), similar depth (~2 m) to Breton Sound and Terrebonne Bay (Reed et al., 1995), two of the other largest embayments, of the MRD. As such, Barataria Bay is both representative of other major systems in the MRD, and covers enough area that it accounts for a substantive fraction of the hydrology of the entire region. We present geochemical tracer data from surface waters in Barataria Bay as one approach for estimating groundwater fluxes. Radon-222 ($t_{1/2}$ = 3.83 d) and its parent, ^{226}Ra ($t_{1/2}$ = 1620 y), are ubiquitous in nature, relatively easy to measure, and both have orders of magnitude higher concentrations in groundwater than surface waters including seawater (Cable et al., 1996a, 1996b). In addition, ^{222}Rn is a conservative gas commonly used for elucidating mass transfer rates at the land–ocean interface (Cable et al., 1996a, 1996b; Dulaiova et al., 2008; Martin et al., 2007). Because radon concentrations in groundwater greatly exceed those of surface

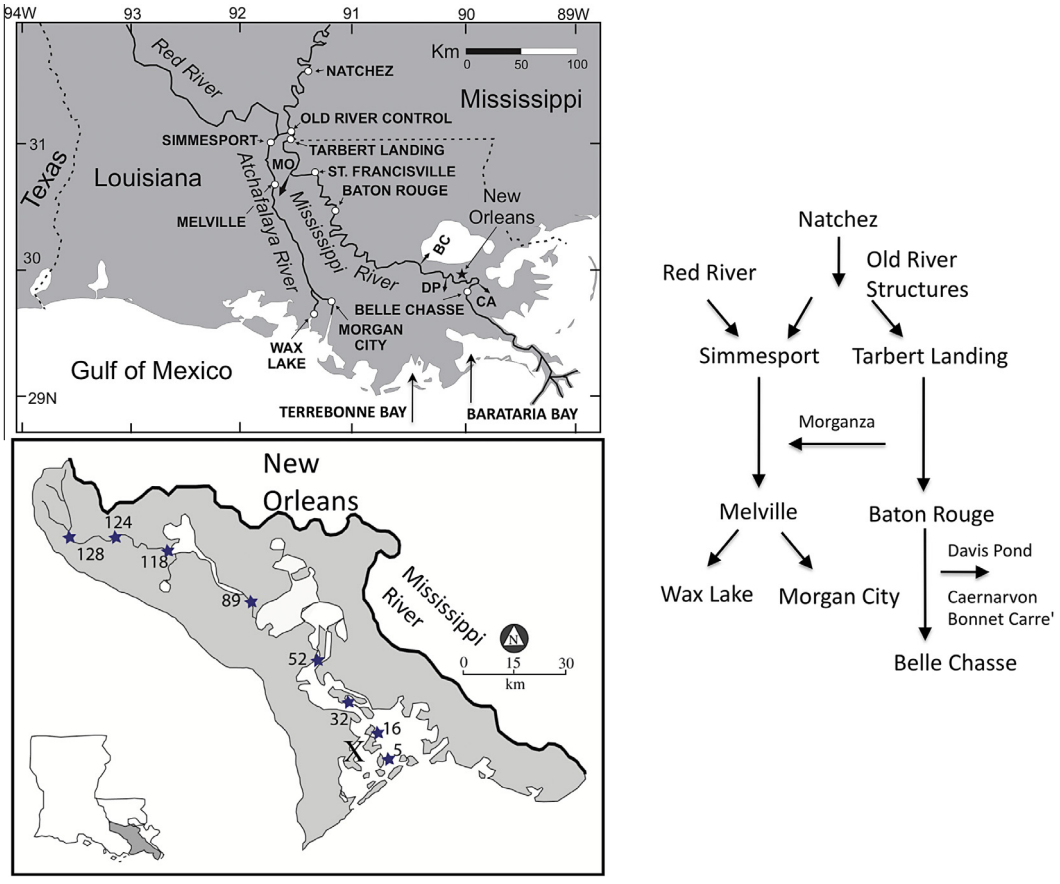

Fig. 1. Top: The lower Mississippi River Delta System, with key stations noted. Bottom: Barataria Bay, with sampling stations used in Fig. 2 noted. The X marks the approximate location of the CHIRP and CRP data. Right: Schematic of water flows in this system, particularly as it pertains to Tables 3 and 4 (modified from Allison et al. (2012).

waters, it can be used to quantify groundwater inputs if all other radon sources and sinks are budgeted.

Eight stations were sampled for water and sediments along a transect from the mouth of Barataria Bay at 5, 16, 32, 52, 89, 118, 124, and 128 km upstream to examine the spatial and temporal variability in ^{222}Rn (Inniss, 2002). This sampling transect was repeated nine times over the period from May 1999 to August 2001 (Fig. 1). Water column samples were analyzed for ^{226}Ra and total ^{222}Rn. Total ^{222}Rn activities were corrected for supported activities using ^{226}Ra and decay-corrected to the time of collection to obtain excess ^{222}Rn. Water column excess ^{222}Rn was then integrated over the depth of the water column to obtain an inventory and subsequently converted to an equivalent flux, J_{inv}, using the decay constant for ^{222}Rn ($\lambda = 0.1809\ d^{-1}$). The total advective flux of ^{222}Rn from sediments, J_{ben}, was estimated using the inventory-derived fluxes, J_{inv}, and after correcting for sediment diffusion and atmospheric evasion (Supplemental Data):

$$J_{ben} = (J_{inv} + J_{atm}) - J_{diff} \quad (1)$$

where J_{atm} is the atmospheric flux of radon gas across the air–sea interface and J_{diff} is the diffusive flux of radon from sediments. Sediment samples were analyzed in sediment equilibration batch slurry experiments (Cable et al., 1996a; Inniss, 2002) to obtain the water column ^{222}Rn that could be supported by sediment diffusion based on the following calculation (Cable et al., 1996a; Inniss, 2002; Martens et al., 1980):

$$J_{diff} = (\lambda D_s)^{0.5} * (C_{eq} - C_o) \quad (2)$$

where J_{diff} is the sediment diffusive flux calculated from measuring C_{eq} in batch experiments; D_s is the bulk sediment diffusion coefficient for radon after correcting the molecular diffusion coefficient, $D_m = 1.14 \times 10^{-5}\ cm^2\ s^{-1}$ (Rona, 1917), for sediment porosity (0.81 ± 0.11) at each station; C_o is the average water column excess ^{222}Rn activity for a given station; and C_{eq} is the average sediment equilibration ^{222}Rn activity assumed to be in equilibrium with sediment pore waters at each station (Inniss, 2002). Atmospheric evasion is a function of mixing in the water column and the solubility of radon in water. We estimate mixing based on the piston velocity, k, at the water surface controlled by wind speed (Wanninkhof et al., 1990). The flux, J_{atm}, of ^{222}Rn gas to the atmosphere is calculated using the following relationship (Broecker and Peng, 1974; Dimova and Burnett, 2011):

$$J_{atm} = k(C_o - \alpha C_{atm}) \quad (3)$$

where again the piston velocity is k (Wanninkhof et al., 1990); α is the temperature-dependent solubility coefficient of radon (Peng et al., 1974) and C_{atm} is the concentration of ^{222}Rn in air, taken as $0.56\ dpm\ L^{-1}$ (Gesell, 1983; Inniss, 2002). Water column ^{222}Rn activities are a function of benthic inputs (groundwater and diffusion), atmospheric evasion, and production and decay in the water column. We correct for production and decay using excess ^{222}Rn. Groundwater inputs, J_{gw}, can then be calculated using the benthic advective flux of ^{222}Rn divided by the mean groundwater activity of ^{222}Rn at the sampling site, C_{gw}:

$$J_{gw} = J_{ben}/C_{gw} \quad (4)$$

The mean groundwater ^{222}Rn activity measured in shallow wells during the 1999–2001 sampling period was $109\ dpm\ L^{-1}$ (range $20–339\ dpm\ L^{-1}$; $n = 6$ wells $\times$ 4 sampling events; (Inniss, 2002).

We complement the geochemical data with hydrologic data on rivers, wells, estuaries, and other water bodies obtained from a variety of published and publically available sources. For information on surface water properties in Barataria Bay, we used reports by local authorities (Reed, 1995). For well data, we employ data from the US Geological Survey's Or-42 well, one of the longest running well records in the region (waterdata.usgs.gov/#295652090020101). To understand tidal exchange at the mouth of Barataria Bay, we used data available from the US Geological Survey (waterdata.usgs.gov/#073802516). To examine the potential for loss of water from the Mississippi River from surface waters to groundwater we examined hydrological fluxes measured at key gauging stations along the Mississippi River. These data are available from the US Geological Survey and the US Army Corps of Engineers, and the processing methods of this dataset are explained in more detail elsewhere (Allison et al., 2012).

To search for potential pathways for subterranean flow in the MRD, we employed geophysical methods to delineate paleochannels and associated freshwater fluxes. Here, both CHIRP sonar and a continuous resistivity profiling (CRP) system were employed (Fig. 1). CHIRP sonar transmits sounds of varying frequencies (typically 2–25 kHz) directed at the sediments, and receives these sonic pulses as the sound waves are reflected off the buried features. Changes in sediment density produce changes in sonic returns, and this information is integrated to produce two dimensional (2D) images of the sediments (LeBlanc et al., 1992). CRP systems work on the principle that sediments with pore space filled by salty marine waters tend to be electromagnetically conductive, whereas sediments with pore space filled with freshwater tend to be more resistive (Breier et al., 2005; Day-Lewis et al., 2006; Evans, 2007; Henderson et al., 2010; Swarzenski et al., 2006). The CRP system consisted of a series of electrodes (Marine Supersting, Advanced Geosciences) that were towed by boat across Barataria Bay, and the continuously recorded data were subsequently converted to a 2D image of sediment resistivity used to infer spatial changes in salinity in sediments and the water column (Breier et al., 2005; Day-Lewis et al., 2006; Evans, 2007; Henderson et al., 2010; Swarzenski et al., 2006). Both the CHIRP and CRP systems were towed across Barataria Bay in October 2009 in the R/V *Grey Goose*, a 7-m research vessel.

4. Results

4.1. Radon geochemistry

Rn-222 fluxes at 8 stations that follow a SE–NW transect across Barataria Bay are labeled by their distance from the mouth of the bay, and the data are presented with the diffusive flux, atmospheric flux (e.g. mixing loss), the total inventory-derived flux, and the net benthic flux (Table 1). The net benthic flux, accounting for mixing losses and sediment diffusion, represents water column ^{222}Rn that cannot be explained except through groundwater discharge. Overall, the ^{226}Ra concentrations (equivalent to the water column supported values) ranged from a low of 0.27 dpm L^{-1} to a high of 2.66 dpm L^{-1}, with a mean ($\pm 1\sigma$) of 0.89 ± 0.53 dpm L^{-1}. The values of excess ^{222}Rn ranged from a low of 0.01 ± 0.12 dpm L^{-1} to a high of 53.1 ± 0.7 dpm L^{-1}, with concentrations averaging 5.98 ± 9.06 dpm L^{-1}.

In general, the greatest ^{222}Rn J_{ben} fluxes were found near the landward edge of the transect in the upper basin, and the lowest ^{222}Rn fluxes were found in the central region of Barataria Basin, whereas moderate ^{222}Rn fluxes were found towards the seaward end of the transect (Table 1; see also Supplemental Data). Rn-222 deficits found in the central bay region in most months are attributed to greater fetch across the open water of the marine lakes system and the increased atmospheric evasion of radon (Inniss, 2002). We estimated the atmospheric evasive flux to be between 0 and 23,000 dpm m^{-2} d^{-1}. Moderate excess ^{222}Rn fluxes near the mouth of Barataria Basin may be attributed to the terminus of an, as yet undiscovered, buried paleochannel. Rn-222 fluxes varied over time as well, with the greatest excess ^{222}Rn fluxes found on December 5, 2000 (27,500 dpm m^2 d^{-1} at the 128 km station) and January 11, 2000 (10,800 dpm m^2 d^{-1} at the 128 km station). Rn-222 deficits were measured (~ -1000 dpm m^2 d^{-1}) on October 6, 1999 and again on June 27, 2000, September 6, 2000 and December 5, 2000 sampling, indicating atmospheric wind evasion is an important sink for radon in this bay.

4.2. Hydrologic data

The distribution of salinity in Barataria Bay also provides insights into potential SGD fluxes in the MRD. Specifically, the most saline waters occur in the southern part of the bay adjacent to the passes (tidal inlets), whereas the freshest waters occur in the north at the upper end of the coastal watershed boundaries (Inoue et al., 2008). The salinity gradient across the bay suggests a large, up-basin source of freshwater, yet direct inputs of river water to these systems are small, in part because a series of levees along the Mississippi River prevents most overland flow (Reed et al., 1995). A freshwater river diversion structure, the Davis Pond Freshwater Diversion (DPFD), operates about midway up the Barataria Basin and is capable of delivering up to 300 m^3 s^{-1} of freshwater to the basin; the diversion delivered an average of 95 m^3 s^{-1} of water to the Barataria Basin during the years 2008–2010 (Allison et al., 2012). The DPFD can have a considerable impact on salinity in Barataria Bay when it is operated at its maximum capacity for prolonged periods of time, which occurred during 2010 as an emergency response to the Deepwater Horizon oil spill (Bianchi et al., 2011a). A few smaller siphons divert river water into Barataria Bay, but given their small size (<57 m^3 s^{-1} at maximum capacity, which is rarely achieved) and the irregularity of their use, they are generally not important to freshwater budgets (Allison et al., 2012).

We calculated a hydrological and salt balance for Barataria Bay, and again found an inconsistency in the hydrological fresh/salt balance (Table 2). The flux of water and salt into and out of an estuary, assuming conservative mixing can be described as:

$$T_{in} * S_{in} = T_{out} * S_{out} \quad (5)$$

where T_{in} is the transport of water entering the estuary on the flooding tide, S_{in} is the salinity of water entering the estuary on the flooding tide, and T_{out} and S_{out} are the transport of water and the salinity of water exiting the estuary on the ebb tide. T_{in} should be equal to the amount of water transported by the tidal prism (T_{tp}). Assuming that the volume of water in Barataria Bay remains in a steady state, then

$$T_{out} = T_{tp} + T_{surf} + T_{rain} + T_{SGD} \quad (6)$$

where T_{surf} is the transport of surface waters (which can be broken down into surface water fluxes with and without the DPFP), T_{rain} is the flux of rainwater to the system, and T_{SGD} is the flux of SGD. Table 2 presents these values and their data sources. These equations were solved for T_{SGD}, and indicate a hydrological flux of 1.48×10^3 m^3 s^{-1} if the DPFD is included in these calculations and 1.57×10^3 m^3 s^{-1} if the DPFD is not included.

To examine the spatial influence of SGD on coastal waters, we developed plots of salinity distributions in surface waters of the northern Gulf of Mexico, using the NGOMNFS model (Ko et al., 2008). This model produces Forecasts/Nowcasts of hydrographic conditions in the northern Gulf of Mexico that are closely coupled to real-time data, producing a realistic picture of conditions for the

Table 1
Estimates of groundwater fluxes to Barataria Basin, Louisiana, are calculated from a radon mass balance.

Distance upstream (km)	J_{inv} (dpm m^{-1} d^{-1})	J_{atm}	J_{diff}	J_{ben}	F_{gw}–q (m s^{-1})	Mean F_{gw}–q (m s^{-1})	Seasonal total ($SGD \times 10^3$ m^3 s^{-1})
5/25/1999							
5	1395	4424	501	5319	5.65E−07	3.07E−07	1.26
16	245	2430	568	2108	2.24E−07		
32	280	2277	1488	1069	1.13E−07		
52	434	2848	1041	2241	2.38E−07		
89	681	3736	1674	2743	2.91E−07		
116	3612		1751	1861	1.98E−07		
124	7969		1247	6722	7.14E−07		
128	2482		1385	1098	1.17E−07		
10/6/1999							
5	392	2137	505	2024	2.15E−07	6.70E−08	0.28
16	163	1634	569	1228	1.30E−07		
32	290	1402	1489	203	2.16E−08		
52	24	160	1045	−860	−9.14E−08		
89	378	3654	1678	2354	2.50E−07		
116	1083		1778	−695	−7.38E−08		
124	1341		1300	41	4.33E−09		
128	2154		1397	757	8.04E−08		
1/11/2000							
5	744	512	503	753	8.00E−08	2.88E−07	1.18
16	1221	1219	560	1881	2.00E−07		
32	144	122	1489	−1223	−1.30E−07		
52	3	2	1045	−1040	−1.10E−07		
89	537	506	1676	−633	−6.72E−08		
116	9356		1724	7631	8.10E−07		
124	4573		1252	3321	3.53E−07		
128	12,346		1316	11,030	1.17E−06		
4/18/2000							
5	3231	5238	500	7969	8.46E−07	3.83E−07	1.57
16	508	3307	566	3249	3.45E−07		
32	1596	2037	1487	2146	2.28E−07		
52	224	1706	1042	888	9.43E−08		
89	869	7175	1669	6374	6.77E−07		
116	5437		1751	3686	3.91E−07		
124	3387		1268	2119	2.25E−07		
128	3834		1378	2456	2.61E−07		
6/27/2000							
5	1983	7677	500	9160	9.73E−07	4.65E−07	1.91
16	1869	7216	564	8521	9.05E−07		
32	76	197	1490	−1217	−1.29E−07		
52	125	603	1043	−316	−3.35E−08		
89	489	7770	1677	6581	6.99E−07		
116	6234		1746	4488	4.77E−07		
124	6177		1272	4905	5.21E−07		
128	4286		1379	2907	3.09E−07		
9/6/2000							
5	890	14,737	503	15,124	1.61E−06	7.51E−07	3.08
16	1657	32,345	565	33,437	3.55E−06		
32	129	2763	1490	1403	1.49E−07		
52	0						
89	24	876	1682	−782	−8.30E−08		
116	1129		1780	−651	−6.91E−08		
124	1225		1300	−75	−7.97E−09		
128	2467		1393	1074	1.14E−07		
12/5/2000							
5	1476	7360	501	8335	8.85E−07	1.16E−06	4.76
16	512	2909	569	2852	3.03E−07		
32	38	868	1490	−584	−6.20E−08		
52	106	2947	1044	2009	2.13E−07		
89	1315	22,692	1672	22,335	2.37E−06		
116	13,596		1695	11,901	1.26E−06		
124	28,818		1121	27,697	2.94E−06		
128	14,274		1301	12,973	1.38E−06		
3/14/2001							
5						6.34E−07	2.60
16							
32	630	1622	1488	764	8.11E−08		
52	391	3892	1041	3242	3.44E−07		
89	1558	8661	1669	8550	9.08E−07		

(*continued on next page*)

Table 1 (*continued*)

Distance upstream (km)	J_{inv} (dpm m^{-1} d^{-1})	J_{atm}	J_{diff}	J_{ben}	F_{gw}–q (m s^{-1})	Mean F_{gw}–q (m s^{-1})	Seasonal total ($SGD \times 10^3$ m^3 s^{-1})
116							
124							
128	12,628		1314	11,314	1.20E−06		
8/21/2001							
5	2880	7156	498	9537	1.01E−06	2.26E−07	9.25
16	769		564	204	2.17E−08		
32	660		1487	−827	−8.79E−08		
52	650	1331	1040	941	9.99E−08		
89	960		1675	−715	−7.60E−08		
116	4793		1755	3037	3.22E−07		
124	3825		1285	2540	2.70E−07		
128	3667		1379	2287	2.43E−07		

Table 2
Missing hydrological fluxes for Barataria Bay.

	Daily flow (m^3 d^{-1})	Instantaneous flow (m^3 s^{-1})
Tidal prism[a]	2.30×10^8	2.66×10^3
Unregulated surface fluxes[a]	1.73×10^7	200
Davis Pond Freshwater Diversion[b]	7.78×10^6	90
Rainwater flux[c]	2.46×10^6	28
Evaporative flux[d]	1.87×10^6	22
Flood tide salinity[e]	25	25
Ebb tide salinity[e]	15	15
Missing hydrological flux with DPFD	1.28×10^8	1.48×10^3
Missing daily hydrological flux without DPFD	1.35×10^8	1.57×10^3

Please note that in some cases the source data was not available with errors; for an evaluation of the sources of variability in these terms, see Tables 3 and 4.

[a] Reed et al. (1995).

[b] Allison et al. (2012).

[c] Calculated from daily rainfall data for New Orleans (nws.noaa.gov), multiplied by the area of the bay (from Feng and Li, 2010).

[d] McCorquodale et al. (2008).

[e] Clear Report: Barataria Pass site from waterdata.usgs.gov.

time and spatial conditions for which they are available (Ko et al., 2008). These conditions are presented for two contrasting periods: a high discharge period on April 15, 2010 when flow of the Mississippi River at Tarbert's Landing, Mississippi immediately downriver of Old River Control was 24.0×10^3 m^3 s^{-1}, and a low discharge period on October 10, 2010, when the flow at Tarbert's Landing was 9.0×10^3 m^3 s^{-1} (Fig. 2). The high flow period shows low salinity conditions in surface waters across the northern Gulf of Mexico, with salient features including: a large plume off of Southwest Pass, an anticyclonic eddy in the Barataria Bight, and fresh conditions in Barataria Bay and Breton Sound. During the low flow period, there are smaller plumes off of Southwest Pass and the other passes of the Mississippi River, a smaller and relatively salty eddy in the Barataria Bight and intermediate to brackish conditions in Barataria Bay and Breton Sound.

Hydrological data for the Mississippi River and its main distributary, the Atchafalaya River are presented in Table 3 as average annual discharge (in 10^9 m^3 y^{-1}= km^3y^{-1}) for water years (e.g., 1 October–30 September) 2008 through 2012. These data were previously published for 2008–2010 (Allison et al., 2012) and have been updated to include water years 2011 and 2012 using the same methods. The total water input to the lower Mississippi River is well described by the flow at Natchez, MS (RK 582), which is downstream of all the major tributaries to this system, whereas the total flow entering the reach of river below the Old River Control Structure is well described by the gauge at Tarbert's Landing (Fig. 1). The total Mississippi + Red River flow entering the Atchafalaya River system is well described by the flow at Simmesport, Louisiana (Fig. 1). Exits from the main Mississippi channel above the Belle Chasse station include the flood control structures at Morganza (used in 2011 only) and Bonnet Carré (used in 2008 and 2011), and annually operated freshwater diversions at Davis Pond (enters Barataria Bay) and Caernarvon (enters Breton Sound). Below Belle Chasse multiple natural and man-made exits are present prior to the main deep-water pass exits to the Gulf of Mexico. The total flow leaving the Atchafalaya River is well described by gauges at Morgan City and the Wax Lake/Calumet outlet immediately landward of Atchafalaya Bay (Allison et al., 2012).

Annual water discharge along the Mississippi River ranged from 489 to 793×10^9 m^3 at Natchez, 371–623×10^9 m^3 at Tarbert's Landing, 376–608×10^9 m^3 at Baton Rouge, and 377–531×10^9 m^3 at Belle Chasse (Table 3). In all cases, the lowest values were measured in 2012 and the highest values were measured in 2010. Annual water discharge at the three major outlets along the main stem of the Mississippi River, the Bonnet Carré Spillway, the Caernarvon Freshwater Diversion, and Davis Pond Freshwater Diversions ranged from 3 to 25×10^9 m^3, with the greatest values measured in 2011, a major flood year when the Bonnet Carré Spillway was opened to remove pressure on levees in New Orleans. In 2011 the Morganza Spillway was also opened to further remove pressure on levees along the main stem on the Mississippi River, diverting 7×10^9 m^3 of water from the Mississippi River to the Atchafalaya River. Along the Atchafalaya River, 207–262×10^9 m^3 of water passed the river's uppermost gauge at Simmesport, 164–262×10^9 m^3 flowed passed Melville, and 159–267×10^9 m^3 of water exited the system through the Wax Lake and Morgan City outlets. As in the Mississippi River, the greatest water discharge occurred in 2010 and the lowest discharge occurred in 2012. Along the Mississippi River, the greatest water losses occurred during the flood year of 2008 (37 km^3, 6.3% of the total flow), whereas water appeared to enter the system during the drought year of 2012 (-10×10^9 m^3, −2.6% of the total flow). Along the Athchafalaya River, water fluxes were much closer to being in balance, with water fluxes ranging from a loss of 3.0×10^9 m^3 (1.2%) in 2008 to water gain of 5.2×10^9 m^3 (−2.0% in 2010).

To develop a more detailed understanding of hydrological fluxes in this system, we examined river discharge during periods of extreme low discharge (9/16/2012–9/30/2012), typical low discharge (11/23/08–12/04/08), moderate discharge (3/27/09–4/06/09), high discharge (5/23/09–6/06/09), and high and rising discharge (4/20/2011–5/4/2011) in Table 4. Whereas conditions in the Mississippi River are constantly changing, these dates correspond to biweeekly-scale periods in the hydrograph that were relatively stable (except for the high and rising period) and do not correspond with periods when flood control exits (e.g., the Morganza and Bonnet Carré Spillways) were operating. During the

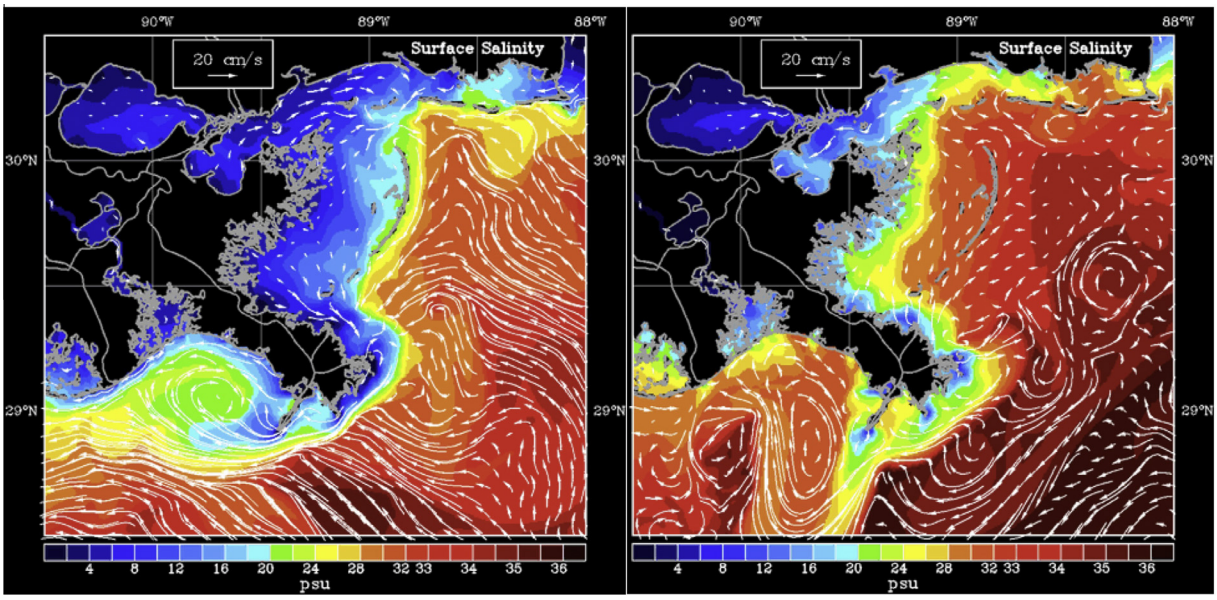

Fig. 2. Salinity in the MRD and its coastal zone from April 15, 2010 (left) and October 10, 2010 (right), with yellow arrow pointing towards Barataria Bay. Source: http://www7320.nrlssc.navy.mil/IASNFS_WWW/NGOMNFS_WWW/NGOMNFS.html. (For interpretation of the references to color in this figure legend, the reader is referred to the web version of this article.)

Table 3
Water discharge ($10^9 m^3 y^{-1}$ = $km^3 y^{-1}$) at gauging stations on the Mississippi and Atchafalaya River for water years 2008–2012. Data sources and methods are described in Allison et al. (2012).

Mississippi River	2008	2009	2010	2011	2012
Natchez	722	611	796	698	489
Natcchez–Old River Control Structure	532	469	623	500	373
Tarbert Landing	578	482	610	519	371
Morganza Spillway	0	0	0	7	0
Baton Rouge	556	474	608	517	376
Bonnet Carre Spillway, Davis Pond, Caernarvon	11	5	6	25	3
Belle Chasse	531	467	595	490	377
Lower River Loss-Tarbert Landing-(BC+BCS, DP, Car)	37 (6.3%)	10 (2.0%)	9 (1.5%)	−4 (−0.01%)	−10 (−2.6%)
Atchafalaya River					
Old River Control Structure	190	142	173	198	116
Simmesport	248	207	262	222	222
Red River (Estimated)	58	65	89	24	107
Melville	247	207	262	223	164
Wax Lake	109	95	126	101	74
Morgan City	136	114	141	129	84
Atchafalaya River Outlets Total	245	209	267	230	159
Total Water Loss Simmesport (+Morgana)Outlets	3.0 (1.2)	−2.2 (−1.1)	−5.2 (−2.0)	−0.5 (−0.2)	−0.8(0.5)

low discharge period, the flow at Tarbert's Landing was $6.2 \pm 0.3 \times 10^3$ m^3 s^{-1} and the flow at Belle Chasse was $6.7 \pm 0.6 \times 10^3$ m^3 s^{-1}, indicating relatively little change in discharge during this period. On the other hand, during the high discharge period the flow at Tarbert's Landing was $35.5 \pm 0.5 \times 10^3$ m^3 s^{-1}, and the flow at Belle Chasse was $30.4 \pm 0.8 \times 10^3$ m^3 s^{-1}, indicating a water loss of about 5.1×10^3 m^3 s^{-1}, or about 14% of the total flow of the lower Mississippi River. During the extreme low discharge period the total flow at Tarbert's Landing was $4.4 \pm 0.2 \times 10^3$ m^3 s^{-1}, while the flow at Belle Chasse was $5.1 \pm 0.4 \times 10^3$ m^3 s^{-1}, suggesting an input of about 0.7×10^3 m^3 s^{-1}. Furthermore, during the high and rising period of discharge, the flow in the river ranged from $24 \pm 3 \times 10^3$ m^3 s^{-1} at Tarberts Landing to $22.2 \pm 2.9 \times 10^3$ m^3 s^{-1}. These data suggest a water loss of $\sim 2 \times 10^3$ m^3 s^{-1}, and the higher variability measured during this period appear to reflect the rising nature of the river stage during this time period. On the Atchafalaya River side, the flow at Simmesport typically matches the combined flow at the Atchafalaya River outlets. For example during the low discharge period, flow was $2.7 \pm 0.4 \times 10^3$ m^3 s^{-1} and the combined flow at the Wax Lake and Morgan City outlets was $2.5 \pm 0.4 \times 10^3$ m^3 s^{-1}, indicating effectively no change in water fluxes during this period. During the high discharge period, the flow at Simmesport was $15.3 \pm 0.4 \times 10^3$ m^3 s^{-1}, and the combined flow at the Wax Lake and Morgan City outlets was $14.7 \pm 0.4 \times 10^3$ m^3 s^{-1}, indicating a minor loss (4%) of 0.65×10^3 m^3 s^{-1}.

4.3. Well data

To directly investigate the role of groundwater in the MRD, we examined the long-term U.S. Geological Survey water-level record of a groundwater well located in New Orleans, LA (Fig. 3; USGS Site # 295652090020101, Orleans Parish). Over year-to-year time scales, the depth to water in this well exhibited 0.5–1.0 m-scale fluctuations that occurred with annual-scale periodicity. Over longer time scales, the OR-42 well shows a decline in water levels from the early 1950s to the late 1960s, which is followed by a

Table 4
Bi-weekly discharges at key gauging stations along the Mississippi and Atchafalaya Rivers during various river stages. Note that values are presented as $\times 10^3$ m^3 s^{-1}. Data is from Allison et al. (2012) and sources therein.

Mississippi River	Very low discharge 9/16/12–/30/12		Low discharge 11/23/08–12/04/08		Medium discharge 3/27/09–04/06/09		High discharge 5/23/09–06/06/09		Rising discharge 4/20/11–5/4/11	
	Q_{avg}	Q^{stdev}	Q_{avg}	Q_{stdev}	Q_{avg}	Q_{stdev}	Q_{avg}	Q_{stdev}	Q_{avg}	Q_{stdev}
Natchez, MS	5.90	1.72	8.94	0.12	25.45	0.59	44.22	958	34.11	3.82
Old River Control	1.55	0.14	2.05	0.22	4.88	0.23	10.03	709	8.77	5.90
Natchez – ORC	4.35	1.72	6.89	0.25	20.57	0.63	34.19	1192	25.34	3.87
Tarbert Landing	4.36	0.19	6.22	0.29	19.79	0.28	35.48	901	24.19	2.99
Baton Rouge	4.52	0.28	6.38	0.23	19.26	187	32.98	492	23.69	2.62
Belle Chasse	5.07	0.39	6.67	0.57	19.31	958	30.43	772	22.18	2.95
Atchafalaya River										
Simmmesport	1.82	0.16	2.74	0.40	8.60	180	15.32	401	10.69	1.34
Melville	2.75	0.15	3.03	0.36	8.72	188	15.24	327	10.65	1.20
Morgan City	0.98	0.21	1.49	0.33	4.62	252	8.53	319	5.76	3.60
Wax Lake	0.87	0.15	1.26	0.24	4.11	119	6.14	147	4.65	3.63
AR Outlets Total	1.85	0.26	2.75	0.41	8.73	279	14.67	352	10.41	5.11

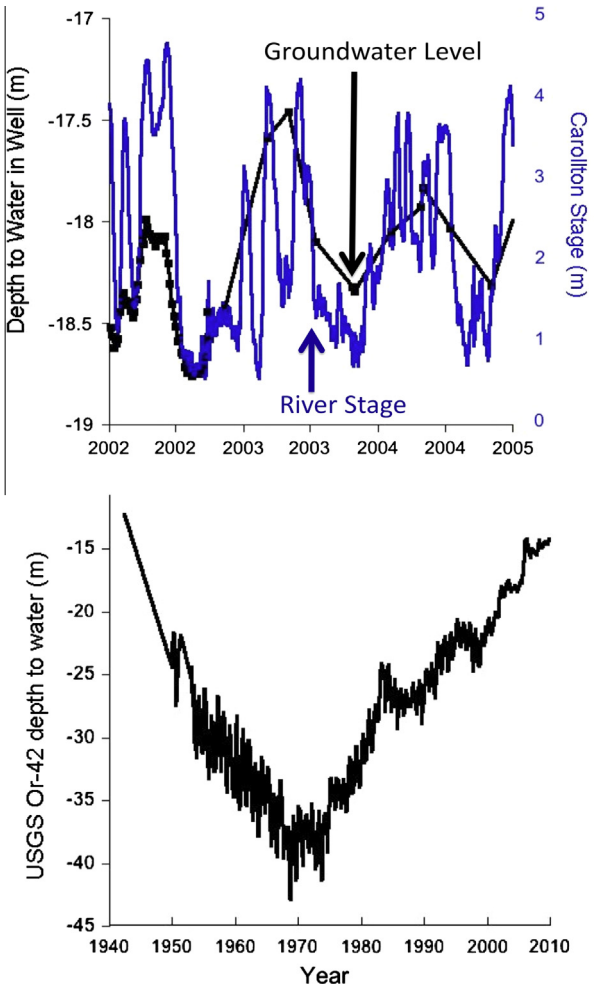

Fig. 3. River stage at New Orleans (Carrollton Gauge) and water levels in USGS OR42 well. Top: Note the temporal coherence between groundwater levels (black) and river stage (blue). This likely indicates that river stage drives groundwater flow, rather than indicating groundwater recharge from rain, as river discharge is primarily driven by precipitation in the Ohio River valley (Meade and Moody 2010). Bottom: Long-term trends in the OR-42 well from 1942 to 2010. (For interpretation of the references to color in this figure legend, the reader is referred to the web version of this article.)

rebound starting in the mid-1970s, and a return to near starting levels by the late 2000s. The highest point on this well record occurred in 1942, when water levels were 12.2 m below the surface, the lowest point on record occurred on September 20, 1968, when water levels reached 42.6 m below the surface. By the late 2000s, water levels had returned to near their original level of ~15 m below the surface. Also plotted here are water levels in the Mississippi River at the Carrollton river gauge in New Orleans. River stage fluctuated between about 0.5 and 4.5 m and was generally highest during the spring freshet and lowest during late summer.

4.4. Geophysical data

A geophysical survey of Barataria Bay was conducted in October 2009 (Fig. 1). The CHIRP sonar image shows sediments with laminations that are cm to dm in scale extending across the Barataria Bay (Fig. 4). These features are interrupted by a zone of unlaminated sediments about 5 m in depth and 350 m in length, and underlain by a hard reflector. The laminated sediments likely represent relatively old river deposits and the bright reflector represents the outline of a channel, lined with coarse-grained sediments that eroded into these deposits. The unlaminated sediments then represent less dense, possibly organic rich deposits, that backfilled this channel, which is a common occurrence in the Mississippi River Delta (Roberts, 1997).

The CRP data reveals patterns of sediment resistivity in pore waters in south-central Barataria Bay (Fig. 4). The most prominent feature in the CRP image is the high resistivity surface water (in blue) overlying the lower resistivity sediments (in warmer colors), with a pronounced transition between the two occurring at the sea floor. Key secondary features include the presence of low resistivity, finger like features, which we interpret as fresh groundwater discharge. These "fingers" are meter scale in depth and 10s–100s of meters in length.

5. Discussion

5.1. A case for groundwater discharge in the Mississippi delta

The presence and nature of SGD inputs to one of North America's most productive ecosystems has been a controversial subject, with conflicting evidence presented by various teams of researchers. Papers by Krest, Moore and colleagues pointed out that concentrations of ^{226}Ra and ^{228}Ra on the Atchafalaya River Shelf, and ^{223}Ra and ^{224}Ra along the Atchafalaya River and Mississippi River shelves, were in excess of what would be expected from the salinity of the system and desorption from bottom sediments, indicating a groundwater source to the system (Krest et al., 1999; Moore and Krest, 2004). On the other hand, a separate study of Ra isotopes on the Mississippi River Shelf west of the MR and south

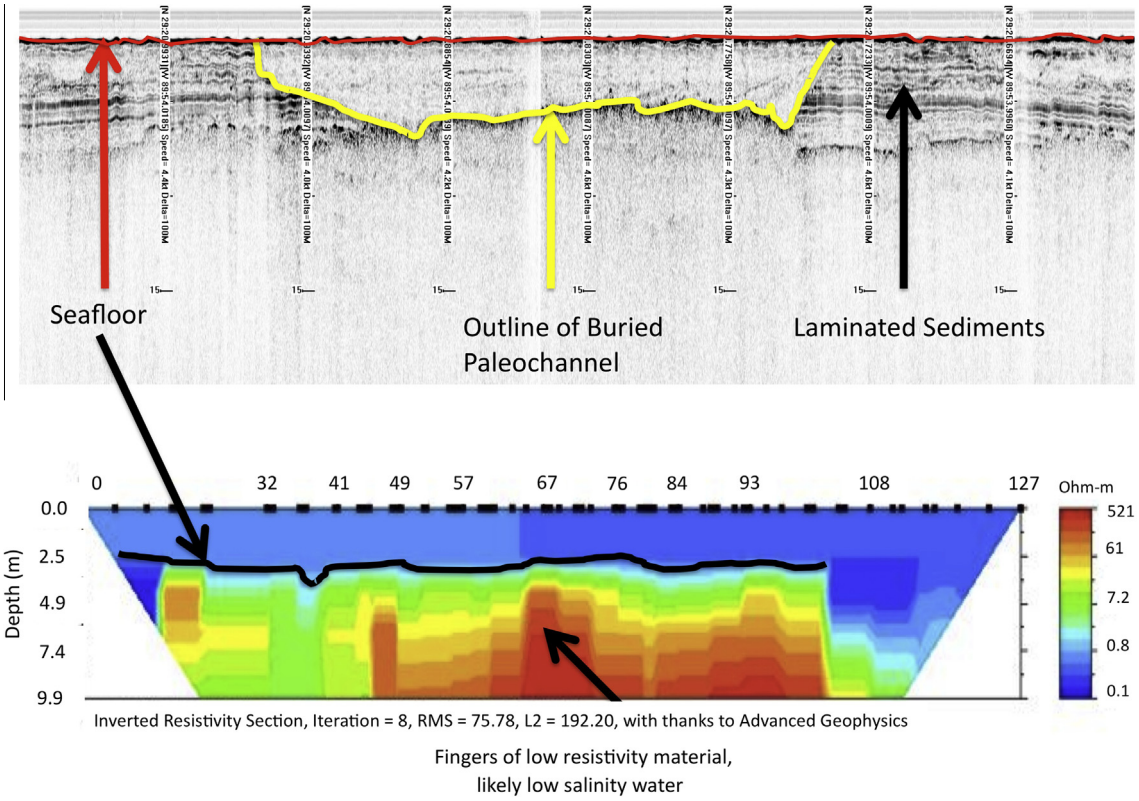

Fig. 4. Geophysical data from Barataria Bay. Top: Chirp image showing channel cut through older laminated strata. Bottom: CRP image showing fingers of low-resistivity water upwelling through the seafloor.

of Barataria Bay found no signal of SGD (McCoy et al., 2007). This lack of detectable SGD was largely attributed to mixing of coastal waters on the continental shelf and the assumption that most of the deltaic muds were of low permeability (McCoy et al., 2007). A modeling study conducted in concert with the McCoy et al. (2007) study indicated that no significant inputs of SGD should occur to the Louisiana continental shelf area due to the anticipated low permeability of deltaic muds (Thompson et al., 2007). Neither of these studies, however, considered the effects of buried sandy paleochannels on SGD in the MRD. Intriguingly, a hydrological model of Barataria Bay that included all known sources of fresh water (i.e., rainfall, overland flow, several small diversions, the Gulf Intracoastal Waterway [GIWW]), found a deficit in the freshwater balance (Inoue et al., 2008). To account for the freshwater deficit, the model suggests the presence of numerous "arbitrary streams" related to overland flow originating from nearby marsh complexes.

We present here a plausible alternate interpretation that can explain all of these studies. Namely that important, previously unidentified groundwater sources exist for the MRD, which are localized and temporally variable. More specifically, results presented above indicate SGD fluxes are associated with paleochannels and other buried sandy bodies, and these SGD fluxes are largely driven by changes in the stage of the Mississippi River. With this view, the differences in groundwater fluxes inferred by the competing Krest and Thompson teams can be attributed to differences in the sampling location with respect to points of groundwater discharge. The arbitrary streams inferred by Inoue et al. (2008) can also be explained by groundwater sources, whereas the lack of SGD reported by the McCoy study may be attributed to the coarse resolution of their model. Our hypothesis is supported by a number of independent lines of evidence that all point to large groundwater inputs to the coastal zone of the MRD.

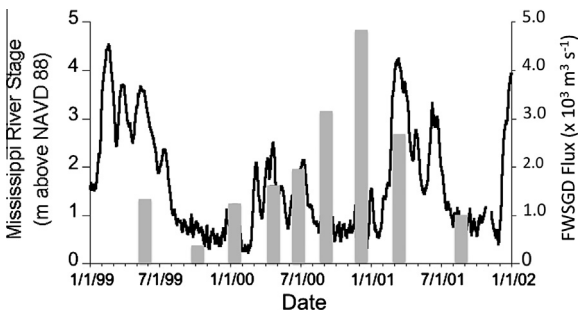

Fig. 5. Seasonal fluxes of fresh SGD in Barataria Bay determined from the distribution of excess ^{222}Rn (grey bars), and the stage of the Mississippi River at New Orleans. Radon data are from Inniss (2002), and stage data are from the US Army Corps of Engineers.

Radon-222 fluxes in Barataria Bay were commonly found to be in excess of that which would be supported from the decay of its parent ^{226}Ra dissolved in the water column and the diffusion of ^{222}Rn from sediments, implying that advective transport, i.e. groundwater flow, is occurring (See Supplemental Data for calculations). Indeed, unsupported fluxes were measured in at least one station during the nine sampling trips to Barataria Bay conducted between May 25, 1999 and August 15, 2001 (Fig. 5). In general, the observation that excess ^{222}Rn fluxes were greatest closest to the river suggests that the hydrological head difference between the river and the surrounding wetlands is at least partially responsible for groundwater flow in this system. The fact that ^{222}Rn fluxes were also observed at the seaward end of the transect is also noteworthy, as it may indicate groundwater flow associated with the termination of Bayou Lafourche, one of the largest and most recent

relict distributaries in the MRD. The timing of the excess ^{222}Rn fluxes is also consistent with a groundwater source driven by river stage (Fig. 5). The lowest ^{222}Rn fluxes were generally found during periods of low discharge, such as October 4, 1999 and September 6, 2000. Interestingly, the greatest excess ^{222}Rn fluxes appear to be associated with periods of rising discharge, and not necessarily the highest discharge. These observations are perhaps consistent with the longer residence time of water in the buried paleochannels relative to the river channel. The resulting radon response to changing stage (e.g., head) would not be observed in the adjacent bays until long after the flood crest (i.e., higher stage) had passed. In addition, at higher river stages the hydraulic head will be greater and groundwater flow should be faster (e.g., shorter residence time), whereas in lower river stages when the hydraulic head is decreased, groundwater flow will be slower and its residence time longer. For shorter residence times, less time is available for radon to accumulate in the groundwater before discharging into the adjacent bay bottom. Alternatively, the resulting response in radon is a hysteresis effect as easily entrained ^{222}Rn is picked up by the groundwater plume early in the seasonal flow, leaving subsequent flows to be slightly ^{222}Rn poor. The process is analogous to those driving suspended sediment transport in the MR, where as river stage increases, easily erodible material is brought into suspension, leaving remaining high waters to be relatively sediment poor (Allison et al., 2012; Snedden et al., 2007). Both explanations are plausible for why radon and river stage do not precisely match all year and further investigation is needed to elucidate this phenomenon.

Groundwater fluxes were calculated Eq. (4) using mean groundwater ^{222}Rn activities collected within the Barataria Basin (Inniss, 2002) and the calculated J_{ben} flux reported here (Supplemental Data). Groundwater discharge varied seasonally and ranged between 0.28×10^3 and 4.76×10^3 m^3 s^{-1} (Fig. 6). Normalized to the area of the basin (4100 m^2), this groundwater would represent about 0.6–10 cm day^{-1}. These fluxes generally follow a seasonal cycle in river stage and are greatest during periods of relatively high river stage and lowest during periods of low river stage. The major exceptions to this pattern occurred during the 9/6/2000 and the 12/05/2001 samplings, which may be influenced by seasonal differences in residence time of groundwater or the hysteresis effect as groundwater plumes entrained radon.

The hydrographic data all point to substantial groundwater transport from the Mississippi River to its delta. The average annual loss of water from the Mississippi River between Tarbert's Landing, MS, and Belle Chasse, LA, above that attributable to the exits shown in Fig. 1, ranges from -10 to 36×10^9 m^3 y^{-1}, or -2.6% to 6.3% of the total annual water flux at Tarbert's Landing. These losses were greatest during 2008, a flood year when the river stage at Baton Rouge reached 13.13 m, close to the maximum of 14.41 m that was reached during the historic flood of 1927 (www.rivergauges.com). Whereas more water was discharged in 2010 than in 2008, 2008 had higher river stages (13.13 m in 2008 vs. 10.66 m in 2010 at Baton Rouge), likely resulting in increased hydrological head driving increased groundwater flow. In contrast, water appeared to enter the system during the drought year of 2012. This input of water in the river is likely the result of the increased influence of tides on the discharge record, which occurs during low river flow, or marine water intrusion into the coastal aquifer.

To understand how this loss of surface water to groundwater varies across the year, we examined the hydrological fluxes in the Mississippi and Atchafalaya rivers at distinct discharges during 1–2 week periods in which the water level was relatively unchanged (Table 4). These periods are long enough to partially account for the water transit time between these locations (2–7 days) and the value exceeds the variability in river flow during this period. Furthermore, tidal effects at the Belle Chasse gauge are accounted for in these calculations, following the approach outlined by Allison et al. (2012). Water loss rates appear to be greatest during high and stable flow periods, which is consistent with the idea of a flow driven pressure gradient associated with the stage differential between the Mississippi River and the surrounding wetlands. For example, during a high flow period in 2009, the average water loss in the Mississippi River was 5.04×10^3 m^3 s^{-1}, equivalent to about 14% of the total flow of the river. These observations contrast with low and moderate flow periods during 2008 and 2009, when no measurable water loss was detected, at least

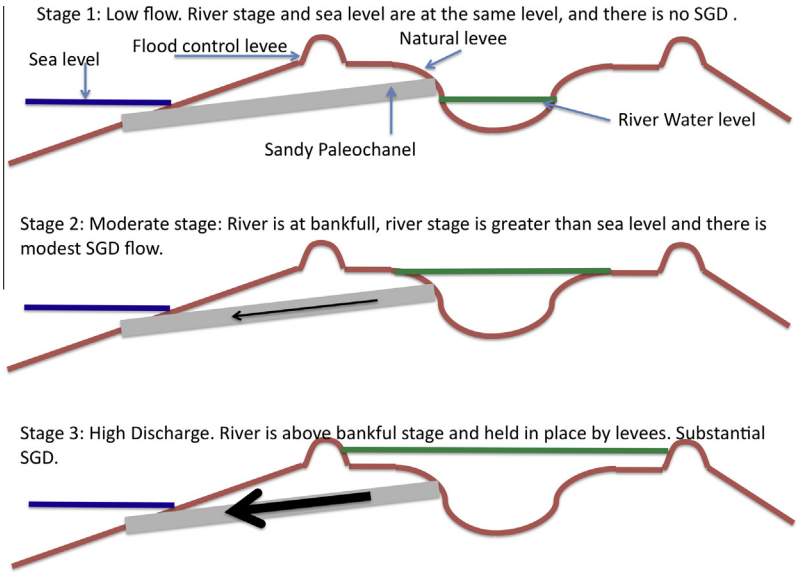

Fig. 6. Schematic of river-impressed SGD in the MRD, envisioned as a three-stage model. During stage 1, the river is at low flow and there is no head differential between the river and the coastal bays, and as such no SGD. During stage 2, the river is at bankful stage and there is a modest head differential between the river and coastal bays, and as such modest levels of SGD. During stage 3, the river is pressing against the levees, and there is a substantial head differential between the river and the coastal bays, and thus a substantial SGD flux.

within the error of the gauges. Furthermore, the period of extreme low discharge in 2012 suggests a water gain of $0.71 \pm 0.39 \times 10^3$ m^3 s^{-1}, which is consistent with the view that marine waters intrude during periods of low discharge. Interestingly, these data do not suggest a water loss from the Atchafalaya River, which is less constrained by levees than the Mississippi River. Furthermore, the quasi-linear shoreline along Louisiana's southwest coast near the Atchafalaya River may reduce pathways for salt water intrusion, whereas the projecting throat of the Mississippi River may promote it. Hydrological data in the Mississippi River suggest an unaccounted for loss of water from the river (Tables 3 and 4), and hydrological data in Barataria Bay suggests a concommitant unaccounted source of freshwater (Table 2) of the same order of magnitude as the water loss in the Mississippi River. These results suggest a missing source of $1.48–1.57 \times 10^3$ m^3 s^{-1} of freshwater in Barataria Bay. If similar amounts were delivered to Terrebonne Bay and Breton Sound, the other large bays in this system would effectively balance the water loss observed in the Mississippi River during high water (Tables 2–4).

Water level data for wells within the MRD indicate a link between stage in the Mississippi River and groundwater levels in the alluvial aquifer (Fig. 3). More specifically, groundwater levels co-vary with the Mississippi River stage measured at New Orleans (Carrollton gauge), suggesting the hydraulic head difference between the river and the adjacent bays do indeed lead to an induced groundwater flow at high river stage. The observed covariance in surface and groundwater levels are not likely to be dominated by recharge from local rainfall, as stage in the lower Mississippi River is largely driven by freshwater inputs in the upper part of the watershed, particularly the Ohio River Valley, which contributes about 40% of the freshwater to the lower Mississippi River (McKee et al., 2004; Meade and Moody, 2010). Interestingly, long-term trends in this gauge are likely driven by the history of water withdrawal in the region (Prakken and Wright, 2009).

Because the MRD is predominantly a muddy system, it might seem paradoxical that large amounts of subsurface flow should occur. However, the architecture of this system can account for the pathways and processes that drive SGD in this system (Fig. 6). We suggest that a hydrological head difference between the river and surrounding wetlands drives groundwater flow through paleochannels and other sandy bodies in the system. In the MRD, a series of natural and artificial levees flank the Mississippi River from near its mouth at Venice, LA for over 3000 km inland. Bankfull stage, which approximates the natural levee height, is 5.18 m in New Orleans and 8.23 m in Donaldsonville, LA, which is the start of Bayou Lafourche, the previous active distributary of the MR. These levees set up a hydraulic gradient between the river and adjacent bays that averages 0.26×10^{-3}–1×10^{-3}, though this number may be greater in systems that are directly next to the river.

Moreover, the MRD is laced with relict distributaries, mouth bars and barrier islands that could serve as conduits for SGD. The possible importance of paleochannels was recognized by Mulligan et al. (2007), who noted that paleochannels along the South Carolina continental shelf could serve as conduits for groundwater flow. We find evidence that coarse-grained paleochannels, mouth bars, and lateral bars all exist in the MRD (Coleman and Prior, 1980), and we hypothesize that these channels can act as conduits for groundwater flow (e.g. Mulligan et al., 2007). For example, Fig. 4 shows a feature that is most likely a relict paleochannel below the seafloor in Barataria Bay. Furthermore, a resistivity profile from a nearby location in Barataria Bay (Fig. 4) indicates low salinity water upwelling from sediments in Barataria Bay. Historical maps of Barataria Bay show a vast network of channels across the bay (Welder, 1955; Fig. 7). A detailed analysis of historical maps suggests that the entire delta plain contained 71 distributary channels before the leveeing of the Mississippi in the 19th and 20th centuries (Syvitski and Saito, 2007). Along the eastern flank of the MRD, several investigators have noted that flow through the Pine Islands

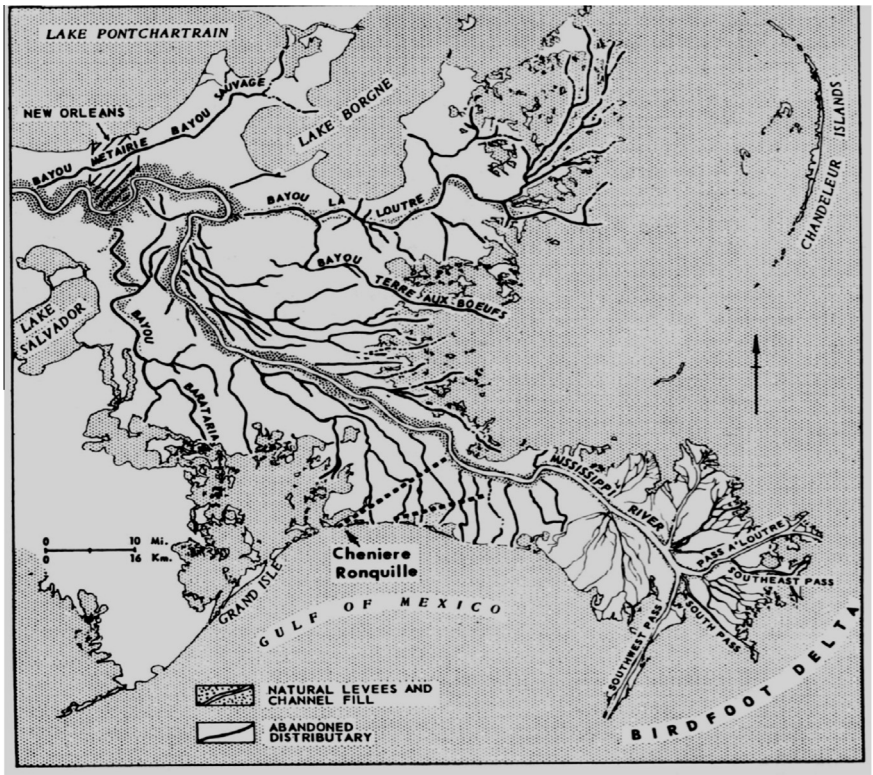

Fig. 7. Paleochannels in the MRD. Source: Welder, 1955.

Table 5
Summary of measured or inferred fluxes of fresh submarine groundwater discharge into the Mississippi River Delta.

Location	Time period	Method	Flux ($\times 10^3$ m^3 s^{-1})	Source
MR, Tarberts Landing to Belle Chasse	2008–2010	MR water budget for high, medium and low flow periods	0–5.05	Allison et al. (2012), as interpreted in this study
MR, Tarbets Landing to Belle Chasse	2008–2011	MR water budget average for 4-year period	0.46	Allison et al. (2012), as interpreted in this study
Barataria Bay	1999–2001	Excess ^{222}Rn Flux	0.28–4.76	Inniss (2002), as interpreted in this study
Barataria Bay	1980–2010	Water Budget	1.48–1.75	Reed et al. (1995), Allison et al. (2012), Feng and Li (2010)
Barataria Bight	1994	^{223,224}Rn	1.00	Moore and Krest (2004)

Sands, impressed by Hurricane Katrina, contributed to the collapse of levees in New Orleans (Dunbar and Britsch, 2008; Nelson and LeClair, 2006). Given the high subsidence rates in the region, coupled with the history of avulsions and high deposition rates (Blum and Roberts, 2012; Kolker et al., 2011; Yun et al., 2012), it is likely that more, as yet unidentified, abandoned distributaries exist below the surface in the MRD. These features will undoubtedly provide pathways of SGD inputs to the coastal bays of the MRD.

Given this geological architecture and data on seasonal changes in surface and groundwater levels, SGD in the MRD will likely follow a seasonal cycle. SGD fluxes will typically be greatest during the winter and spring months when river stages, and the hydraulic gradient, are typically at their greatest. Conversely, SGD fluxes will be at their least during late summer and fall, when river stages are at their lowest. These predictions are consistent with the ^{222}Rn-derived fluxes and the water budgets, with the notable caveat that differences in groundwater residence time between high river stages and low river stages, and the lag in response to changing river stage, may create a hysteresis-like response in radon fluxes. Furthermore, during times of low flow, it is possible that salt-water intrusion may occur in these estuarine and deltaic systems.

Overall, findings from this study suggest a total SGD flux to the MRD with an order of magnitude of about 1.0×10^3 m^3 s^{-1} (Table 5). The water budget for the lower MR system for the years 2008–2012 suggests annual SGD fluxes range from -0.30×10^3 to 1.16×10^3 m^3 s^{-1}. Periods of high flow may yield SGD fluxes as high as 5.05×10^3 m^3 s^{-1}, whereas periods of low flow may experience recharge/marine water intrusions of $0.71 \pm 0.39 \times 10^3$ m^3 s^{-1}. A water budget for Barataria Bay implies an SGD flux of $1.28–1.35 \times 10^3$ m^3 s^{-1}, whereas excess Rn fluxes in the bay indicates the SGD flux ranges between 0.28 and 4.76×10^3 m^3 s^{-1}. Given that Barataria Bay occupies about 20% of the entire area of the MRD, these "bayside" values compare reasonably well to the "riverside" values. In comparison, Moore and Krest (2004), who studied SGD in the Barataria Bight, which is west of the lower MR, estimated an SGD flux of about 1000 m^3 s^{-1} in 1994. Our study suggests that SGD fluxes in the MRD range between 0% and 15% of the total flow in the MR, whereas Moore and Krest (2004) suggested SGD fluxes to the Barataria Bay were about 7% of the total flow of the MR at the time they sampled. The water budget and radon mass balance estimates of SGD here agree remarkably well, and are effectively in line with literature values (e.g. Moore and Krest 2004), indicating that groundwater may indeed be the missing water source in previous hydrodynamic models (e.g. Inoue et al., 2008).

Values of SGD can also be compared to surface water fluxes in the MRD. According to Reed et al. (1995), the average surface flows to Barataria and Terrebonne Bays are 0.16×10^3 m^3 s^{-1} and 0.13×10^3 m^3 s^{-1} (Table 3), suggesting that the total groundwater flux to coastal bays in the MRD is greater than the surface flux. Whereas this assertion might seem unreasonable at first, it should be noted that surface water fluxes in the MRD have largely been eliminated by a series of levees that extend from near the river mouth to several thousand km inland. Under natural conditions, crevasses along the MR carried volumes of water that regularly exceeded 1.50×10^3 m^3 s^{-1} (Reed et al., 1995; Wells and Coleman, 1987). Further work, including modeling studies coupled with paleooceanographic proxies are clearly needed to fully understand the role of SGD in a natural MRD.

The distribution of SGD fluxes in the MRD is likely to differ substantially from other systems. For example, in karstic coastal aquifers, such as those of Florida, SGD fluxes are typically shore-normal (Burnett et al., 2006; Santos et al., 2009). Shallow sandy coastal aquifers are relatively simple systems where the flux of SGD is also largely considered to be shore-normal (Martin et al., 2007), though recent research suggests that heterogeneity in the geological architecture leads to heterogeneity in the SGD fluxes (Michael et al., 2011). In deltaic settings, like the MRD, the geometry of SGD is likely far more complex. This flow could discharge laterally, normal to the main axis of the channel, or vertically, at the end of a channel. Thus, given the complex distribution of channel networks in the MRD, groundwater may be discharging in many directions, depending on the paths and sinuosity of the channels in the system, and alignment of sediments within and beside the channel.

5.2. Significance of deltaic SGD

5.2.1. Local and regional significance

These findings have important implications for the biogeochemistry of North America's largest delta and its associated shelf and estuarine features. Surface flows from the MR account for ~60% of the total suspended load and 66% of the total dissolved load delivered from the North American continent to the global ocean (Meade, 1996). As a result, as MR waters enter the deltaic subterranean estuary, they undergo a myriad of chemical changes that ultimately affect the composition of waters delivered to the coastal ocean. Subterranean estuaries can serve as locations where dissolved nutrients are remineralized or utilized, and thus can serve as a location for both denitrification and ammonification (Burnett et al., 2006, 2003; Kroeger and Charette, 2007). The deltaic subterranean estuary can also serve as a region where trace elements and contaminants are cycled (Charette and Sholkovitz, 2006; Roy et al., 2011). This metal cycling is likely to occur when Fe-oxides and Fe-sulfides are formed or dissolved, a process that is commonly associated with pulses of organic carbon (Charette and Sholkovitz, 2002; Roy et al., 2010). In the deltaic subterranean estuary, such pulses would be coupled to fluxes of river water, likely rich in DOC (Bianchi et al., 2011a, 2004) through paleochannels during high river stage or through salt water intrusion during low river stage. Finally, changes in the pore water salinity in sediments of the deltaic subterranean estuary can lead to the adsorption and desorption of numerous ions, in a manner analogous to similar processes in surface waters (Charette et al., 2005; Rouxel et al., 2008).

One area where the deltaic subterranean estuary may play a particularly important role is in the cycling of carbon and nutrients in the northern Gulf of Mexico. The surface waters of the MR deliver about 3.1×10^{12} g of DOC to the coastal ocean, which amounts to about 1.2% of the global DOC flux from rivers to the coastal ocean (Bianchi et al., 2004). The composition of DOC along the Mississippi River shelf are generally depleted in terrestrial biomarkers, and several investigators (Bianchi et al., 2009, 2004) have speculated that this is the result of metabolic pathways in the coastal zone. The deltaic subterranean estuary may serve as a conduit for reactive transport during which such metabolic reactions occur. Fluxes of carbon and nutrients play a major role in the development of the hypoxic zone that develops seasonally in the northern Gulf of Mexico (Rabalais et al., 2002). However, models of the hypoxic zone do not yet fully predict its size and magnitude (Forrest et al., 2011; Swarzenski et al., 2006; Turner et al., 2006), and it is possible that SGD may play an important role in nutrient and carbon fluxes into the coastal zone; depending on the flow paths and sediments through which groundwaters pass (Burnett et al., 2003). More detailed analyses of SGD in the MRD may lead to an improved understanding of the development of this hypoxic zone.

Groundwater inputs may also have implications for the ecology of the MRD. The distribution of many plants, birds, fish and shellfish in the MRD are influenced by local salinity, in addition to factors such as flooding periodicity, nutrient availability, and sediment type (Lane et al., 2007; Sklar and Browder, 1998). An enhanced understanding of SGD fluxes to the coastal bays of the MRD could potentially help explain patterns of diversity and abundance of many of these organisms. Because the MRD is one of the most productive habitats for many of these species, an improved understanding of the distribution of SGD could have important broader ecological and economic implications (Day et al., 2007).

Finally, SGD dynamics may be further impacted by climate change (Gallardo and Marui, 2006; IPCC, 2007), as precipitation changes may alter the stage of the Mississippi River, while sea level rise could increase salt water intrusion into the coastal aquifer (Mitsch and Hernandez, 2013; Werner et al., 2013). Given that global sea level rise is accelerating and impacting coastal systems (Church and White, 2006; Kolker et al., 2010), more research is clearly needed to understand how subterranean flow paths and nutrient delivery to the ocean will change during this century.

5.2.2. Applied significance of deltaic SGD

Understanding SGD in large deltas is critically important for society as a whole, as deltas commonly serve as major population centers and conduits for commerce (Day et al., 2007; Syvitski and Saito, 2007). The MRD typifies these relationships between humankind and deltas – it produces vast quantities of seafood, serves as a transportation hub, houses complex industries, and is home to unique cultures (LACPRA, 2012). Restoring the MRD relies, in large part, on restoring the hydrology of the region (Allison and Meselhe, 2010; Kolker et al., 2012; LACPRA, 2012), and as such, it is critical to account for all hydrological fluxes (Allison et al., 2012). Furthermore, groundwater flows in the MRD have important implications

Table 6
Properties of Major Rivers and Their Deltas. Legend: Q = annual water discharge ($km^3\ yr^{-1}$), S = annual sediment discharge ($\times 10^6$ tons yr^{-1}), Delta Area (km^2), Mean GS = Mean grain size (mm); #Ch = number of distributary channels (pre-dam); ChW = channel width (km); TC:RC ratio of total channel width to the width of the main channel; drainage area ($\times 10^6\ km^2$). "–" = no data. Data source: Q and drainage area are from McKee et al. (2004), all else Syvitski and Saito (2007) and Syvitski et al. (2005) except where noted as: *Kolker interpretation of Google Earth Imagery, # = Walker (1998).

River	Country	Delta type	Q	Q Rank	S	S Rank	Delta area	Area rank	Mean GS	# Ch	ChW	TC:RC	Drainage area
Amazon	Brazil	River/ Tides	6300	1	1150	1	467,100	1	30	9	71	8.9	6.15
Congo	Congo	No Delta*	1250	2	43	20	0	25	–	1			3.82
Orinoco	Venezuela	River/ Tides	1200	3	150	10	35,642	6	–	24	28.4	15.8	0.99
Ganges/ Brahmaputra	Bangladesh	Tides/ River	970	4	1050	2	105,641	2	160	32	85.5	28.5	1.48
Yangtze	China	Tides	900	5	480	3	35,000	7	50	4	30	15	1.94
Yenisey	Russia	River/ Tides*	630	6	5	28	4500	21	–	5*			2.58
Mississippi	USA	River	530	7	210	6	38,568	5	10	71	17.9	10	3.27
Lena	Russia	River/ Ice	510	8	11	26	24,000	10	–	115	135.8	17	2.49
Mekong	Vietnam	Wave/ River	470	9	160	8	49,000	3	100	9	17	17	0.79
Parana/Uruguay	Brazil	River/Geol	470	10	100	13	12,975	14	–	12	6.1	6.1	2.83
St. Lawrence	Canada	No Delta	450	11	3	29	0	26	–		NA	NA	1.03
Irrawaddy	Myanmar	Tides	430	12	260	4	30,570	8	50	17	25.8	23.2	0.43
Ob	Russia	River/Ice*	400#	13	16#	25	42,900#	4		2	–	–	2.99
Amur	Russia	No delta*	325	14	52	18	–	–	–	–	–		1.86
Mackenzie	Canada	Ice	310	15	100	14	13,000	13	200	23	10.2	4.5	1.81
Pearl (China)	China	Geol	300	16	100	15	5200	19	–	12	23.8	26.4	0.44
Salween	Myanmar	River/ Tides*	300	17	80	16	Not well described		–	–	–		0.28
Volga	Russia	River	259	18	25.5	23	5400	18	–	85	3	1.7	1.36
Columbia	USA	No Delta	250	19	8	27	0	27	–		NA	NA	0.67
Indus	Pakistan	Tides	240	20	220	5	7500	16	–	7	0.7	1.7	0.24
Magdalena	Colombia	Geological	240	21	50	19	6780	17	–	9	19.3	19.3	0.97
Zambezi	Mozambique	Wave	220	22	20	24	13,920	12	–	4*			1.2
Danube	Romania	Wave	210	23	40	21	4200	23	–	7	1.1	3.7	0.81
Yukon	USA	Wave	195	24	60	17	5200	20	–	43	22.6	5.8	0.84
Niger	Africa	Wave/ Tide	190	25	40	22	17,135	11	150	15	16.9	8.5	1.21
Purari/Fly	New Guinea	TIdes	150	26	110	12	2800	24	–	5	55	36.7	0.09
Red (Hunghe)	Vietnam	River	120	27	160	9	11,400	15	–	10	18.5	4.9	0.12
Nile	Egypt	Wave	110	28	118	11	24,512	9	30	15	1.4	1.9	
Godavari	India	Wave	92	29	170	7	4400	22	–	7	9.6	12	0.31

for engineering geology as fluid flow through buried sand bodies contributed to levee failures during Hurricane Katrina (Nelson and LeClair, 2006; Rogers et al., 2008) and hundreds of sand boils were reported along the lower MR during the flood of 2011 (www.dotd.la.gov). In other systems such as the Ganges–Brahamaputra and Red River deltas, groundwater flow through paleochannels is linked to high concentrations of As and is an important public health threat (Jessen et al., 2008; Michael and Voss, 2009; Rao et al., 2005; Weinman et al., 2008). Thus, groundwater flows need to be considered in management plans of the MRD and other large deltas.

5.2.3. Global significance

To examine the potential global significance of deltaic SGD, a database of the 25 highest-discharging rivers on Earth were compared to a database of global deltas (Table 6). The list of rivers comes primarily from McKee et al. (2004), whereas the list of deltas and their properties comes primarily from Syvitski and Saito (2007), with other sources used to fill in data gaps (e.g. Walker, 1998). Of these 25 largest rivers, all but three have deltas at their mouth, the Congo/Zaire, the St Lawrence, and the Columbia, which have estuaries at their mouth. These 22 large rivers with deltas drain 37×10^6 km^2 of land collectively, amounting to 25% of the total continental land area (149×10^6 km^2). When smaller rivers with large drainage basins and deltas are added to this figure, (e.g. the Nile River Delta), these values increase.

Most of the deltas found at the mouths of these 22 large rivers have extensive channel networks, with the number of distributaries ranging from a low of 4 in the Yangtze River Delta to a high of 115 channels in the Lena River Delta (Table 6). The width of these channels at the shoreline averages 30.3 km and ranges from a low of 1.1 km in the Danube River Delta to a high of 135.8 km in the Lena River Delta. Equally important is the total width of these channels at the shoreline, which is typically much greater than the width of the main stem, with the ratio between the two averaging 12.5 and ranging from a low of 1.7 in the Magdelena River Delta to a high of 28.5 in the Ganges–Brahamputra River Delta. These data indicate that particle size varies considerably between deltas, with average particle sizes ranging from a low of 10 mm in the Mississippi River Delta to a high of 200 mm in the Mackenzie River Delta (Syvitski and Saito, 2007). The data suggest the presence of a worldwide network of buried paleochannels in deltas that could act as conduits for SGD (Table 4), and deltas may be more important than previously understood as a geochemical pathway.

Existing studies of deltaic SGD have demonstrated this geochemical importance for a few elements (Sr, Si). Basu et al. (2001) show that the Ganges–Brahamaputra delta is an important source of Sr to the world's ocean. Specifically, SGD fluxes could account for a substantial amount of the increase in the Sr isotopic ratio of seawater over the past 40 million years (Basu et al., 2001). However, others have argued that these values are both unreasonably high and unreasonably low (Charette and Sholkovitz, 2006; Harvey, 2002). Studies from the Yellow River Delta and the associated Yellow Sea indicate SGD from this system is an important source of Si to the world's ocean, amounting to $4–24 \times 10^9$ mol y^{-1}, whereas the global riverine flux of Si is 23×10^9 mol y^{-1} (Kim et al., 2005). Other studies indicate that the stratigraphy of deltas play an important role in the concentration and distribution of soluble elements in deltas. For example, the distribution of paleochannels plays an important role in the distribution of As in the Ganges–Brahamaputra Delta and Red River Deltas (Acharyya, 2005; Jessen et al., 2008).

Indeed, it should not be surprising that deltas would have important groundwater sources of dissolved constituents. Deltas are one of the major reservoirs for sediments, nutrients and carbon globally. They also serve as a locus for authigenic mineral formation. Many previous studies have focused on SGD along transgressive shorelines, and the next decade is likely to witness an expansion of SGD studies to more complex deltaic systems (Taniguchi et al., 2008) to address this major uncertainty in global hydrological budgets (Moore, 2010; Vaux, 2011; Zekster and Loaiciga, 1993).

Acknowledgements

This work was funded in part by a collaborative National Science Foundation project to Kolker (EAR-1141716), Cable (EAR-1141685), and Johannesson (EAR-1141692), and a Grant from the Coastal Restoration Enhancement Through Science and Technology to Allison and F. Marcantonio (Texas A&M University). Radon data were collected through a grant from the Louisiana Board of Regents (LEQSF-1998-01-RD-A-03) to Cable.

Appendix A. Supplementary material

Supplementary data associated with this article can be found, in the online version, at http://dx.doi.org/10.1016/j.jhydrol.2013.06.014.

References

Acharyya, S.K., 2005. Arsenic levels in groundwater from Quaternary alluvium in the Ganga Plain and Bengal Basin, Indian subcontinent: insights into influence of stratigraphy. Gondwana Res. 8 (1), 55–66.
Aller, R.C., Blair, N.R., 2004. Early diagenetic remineralization of sedimentary organic C in the Gulf of Papua deltaic complex (Papua New Guinea): net loss of terrestrial C and diagenetic fractionation of C isotopes. Geochemica et Cosmochemica Acta 68 (8), 1815–1825.
Allison, M.A. et al., 2012. A water and sediment budget for the lower Mississippi–Atchafalaya River in flood years 2008–2010: implications for sediment discharge to the oceans and coastal restoration in Louisiana. J. Hydrol. 432–433, 84–97.
Allison, M.A., Meselhe, E.A., 2010. The use of large water and sediment diversions in the lower Mississippi River (Louisiana) for coastal restoration. J. Hydrol. 387, 346–360.
Basu, A.R., Jacobsen, S.B., Poreda, R.J., Dowling, C.B., Aggarwal, P.K., 2001. Large groundwater strontium flux to the oceans from the Bengal basin and the marine strontium isotope record. Science 293, 1470–1473.
Basu, A.R., Jacobsen, S.B., Poreda, R.J., Dowling, C.B., Aggarwal, P.K., 2002. Respone to Harvey (2002), "Groundwater flow in the Ganges Delta". Science 296, 1563A.
Berner, E.K., Berner, R.A., 1996. Global Environment: Water, Air, and Geochemical Cycles. Prentice Hall, New Jersey.
Bianchi, T.S., Allison, M.A., 2009. Large-river delta-front estuarise as "recorders" of global environmental change. Proc. Natl. Acad. Sci. 106 (20), 8085–8092.
Bianchi, T.S. et al., 2011. Impacts of diverted freshwater on dissolved organic matter and microbial communities in Barataria Bay, Louisiana, U.S.A. Mar. Environ. Res. 72, 248–257.
Bianchi, T.S., DiMarco, S.F., Smith, R.W., Schreiner, K.M., 2009. A gradient of dissolved organic carbon and lignin from Terrebonne-Timbalier Bay estuary to the Louisiana shelf (USA). Mar. Chem. 117 (1–4, Sp Iss S1), 32–41.
Bianchi, T.S., Filley, T.R., Dria, K., Hatcher, P.G., 2004. Temporal variaiblity in sources of dissolved organic carbon in the lower Mississippi River. Geochim. Cosmochim. Acta 68 (5), 959–967.
Bianchi, T.S. et al., 2011. Sources of terrestrial organic carbon in the Mississippi River plume region: evidence for the importance of coastal marsh inputs. Aquat. Geochem. 17, 431–456.
Blum, M.D., Roberts, H.H., 2012. The Mississippi delta region: past, present and future. Annu. Rev. Earth Planet. Sci. 40, 655–683.
Breier, J.A., Breier, C.F., Edmonds, H.N., 2005. Detecting submarine groundwater discharge with synoptic surveys of sediment resistivity. Geophys. Res. Lett., 32.
Broecker, W.S., Peng, T.H., 1974. Gas exchange rates betweeen air and sea. Tellus 26 (1–2), 21–35.
Burdige, D.J., 2005. Burial of terrestrial organic matter in marine sediments: a re-assessment. Global Biogeochem. Cycles 19, GB4011.
Burnett, W.C. et al., 2006. Quantifying submarine groundwater discharge in the coastal zone via multiple methods. Sci. Total Environ. 367, 498–543.
Burnett, W.C., Bokeniewicz, H., Huettel, M., Moore, W.S., Taniguchi, M., 2003. Groundwater and pore water inputs to the coastal zone. Biogeochemistry 66, 3–33.
Burnett, W.C., Taniguchi, M., Oberdorfer, J.A., 2001. Measurement and significance of the direct discharge of groundwater into the coastal zone. J. Sea Res. 46, 109–116.

Cable, J., Bugna, G., Burnett, W., Chanton, J., 1996a. Application of ^{222}Rn and CH_4 for assessment of groundwater discharge to the ocean. Limnol. Oceanogr. 41, 1347–1353.

Cable, J., Burnett, W., Chanton, J., Weatherly, G., 1996b. Estimating groundwater discharge into the northeastern Gulf of Mexico using radon-222. Earth Planet. Sci. Lett. 144, 591–604.

Charette, M.A., Sholkovitz, E.R., 2002. Oxidative precipitation of groundwater-derived ferrous iron in the subterranean estuary of a coastal bay. Geophys. Res. Lett., 29.

Charette, M.A., Sholkovitz, E.R., 2006. Trace element cycling in a subterranean estuary: Part 2. Geochemistry of the pore water. Geochim. Cosmochim. Acta 70, 811–826.

Charette, M.A., Sholkovitz, E.R., Hansel, C., 2005. Trace element cycling in a subterranean estuary: Part 1. Geochemistry of the permeable sediments. Geochim. Cosmochim. Acta 69, 2095–2109.

Charette, M.A., Spilvalio, R., Herbold, C., Bollinger, M.S., Moore, W.S., 2003. Salt marsh submarine groundwater discharge as traced by radium isotopes. Mar. Chem. 84 (1–2), 113–121.

Church, J.A., White, N.J., 2006. A 20th century acceleration in global sea-level rise. Geophys. Res. Lett. 33 (1).

Coleman, J.M., Prior, D.B., 1980. Deltaic Sand Bodies. Tulsa, OK.

Coleman, J.M., Roberts, H.H., Stone, G.W., 1998. The Mississippi River Delta: an overview. J. Coastal Res. 14 (3), 698–717.

Day, J.W. et al., 2007. Restoration of the Mississippi Delta: lessons from Hurricanes Katrina and Rita. Science 315 (5819), 1679–1684.

Day, J.W., et al., 2012. Answering 10 Fundamental Questions about the Mississippi River Delta, Mississippi River Delta Science and Engineering Special Team.

Day-Lewis, F.D., White, F.A., Johnson, C.D., Lane, J.W., 2006. Continuous resistivity profiling to delineate submarine groundwater discharge - examples and limitations. Lead. Edge, 724–728, June.

Dimova, N.T., Burnett, W.C., 2011. Evaluation of groundwater discharge into small lakes based on the temporal distribution of radon-222. Limnol. Oceanogr. 56 (2), 486–494.

Dulaiova, H., Bonneea, M.E., Henderson, P.B., Charette, M.A., 2008. Chemical and physical sources of radon variation in a subterranean estuary – implications for radon groundwater end-member activities in submarine groundwater discharge studies. Mar. Chem. 110, 120–127.

Dulaiova, H. et al., 2006a. Assessment of groundwater discharges into West Neck Bay, New York, via natural tracers. Cont. Shelf Res. 26, 1971–1983.

Dulaiova, H., Burnett, W.C., Wattayakorn, G., Solisuporn, P., 2006b. Are groundwater inputs into river dominated areas important? The Chao Phraya River- Gulf of Thailand. Limnol. Oceanogr. 51, 2232–2247.

Dunbar, J.B., Britsch, L.D., 2008. Geology of the New Orleans and the Canal Levee Failures. J. Geotech. Geoenviron. Eng. 134 (5), 566–592.

Dunn, D.D., 1996. Trends in Nutrient Inflows to the Gulf of Mexico from Streams Draining the Conterminous United States 1972–1993. 96–4113, USGS, Austin, TX.

Esposito, C.R., Georgiou, I., Kolker, A.S., 013. Efficient delivery of sediment through an active crevasse splay. Geophys. Res. Lett. 40, 1540–1545.

Evans, R.L., 2007. Using CSEM techniques to map the shallow section of seafloor: from the coastline to the edges of the continental slope. Geophysics 72, WA105–WA116.

Feng, Z., Li, C., 2010. Cold-front-induced flushing of the Louisiana Bays. J. Mar. Syst. 82, 252–264.

Forrest, D.R., Hetland, R.D., DiMarco, S.F., 2011. Multivariable statistical regression models of the areal extent of hypoxia over the Texas-Louisiana continental shelf. Environ. Res. Lett. 6 (4), 0450002.

Gallardo, A.H., Marui, A., 2006. Submarine groundwater discharge: an outlook of recent advances and current knowledge. Geo-Mar. Lett. 26, 102–113.

Georg, R.B., West, A.J., Basu, A.R., Halliday, A.N., 2009. Silicon fluxes and isotope composition of direct groundwater discharge into the Bay of Bengal and the effect on the global ocean silicon isotope budget. Earth Planet. Sci. Lett. 283, 67–74.

Gesell, T.F., 1983. Background atmospheric Rn-222 concentrations outdoors and indoors: a review. Health Phys. 45, 289–302.

Harvey, C.F., 2002. Groundwater flow in the Ganges Delta. Science 296, 1563A.

Henderson, R.D. et al., 2010. Marine electrical resistivity imaging of submarine groundwater discharge: sensitivity analysis and application in Waquoit Bay, Massachusetts, USA. Hydrogeol. J. 18 (1), 173–185.

Inniss, L.V., 2002. Scientific and Management Perspectives in Wetland Groundwater Hydrology, Ph.D. Dissertation, Louisiana State University, Baton Rouge, 183 pp.

Inoue, M., Park, D., Justic, D., 2008. A high-resolution integrated hydrology-hydrodynamic model of the Barataria Basin system. Environ. Modell. Softw. 23 (9), 1122–1132.

IPCC, 2007. Climate Change 2007: The Physical Science Basis. Contributions of Working Group I to the Fourth Assessment Report of the Intergovernmental Panel of Climate Change. Cambridge University Press, New York, NY, 996 pp.

Jessen, S. et al., 2008. Paleo-hydrological control on groundwater As levels in Red River delta, Vietnam. Appl. Geochem. 23, 3116–3126.

Johannesson, K.H., Chevis, D.A., Burdige, D.J., Cable, J.E., Martin, J.B., Roy, M., 2011. Submarine groundwater discharge is an important net source of light and middle REEs to coastal waters of the Indian River Lagoon, Florida, USA. Geochimica et Cosmochimica Acta 75, 825–843.

Kim, G., Ryu, J.W., Yang, H.S., Yun, S.T., 2005. Submarine groundwater discharge (SGD) into the Yellow Sea revealed by ^{228}Ra and ^{226}Ra isotopes: implications for global silicate fluxes. Earth Planet. Sci. Lett. 237, 3047–3054.

Ko, D.S., Martin, P.J., Rowley, C.D., Preller, R.H., 2008. A real-time coastal ocean prediction experiment for MREA04. J. Mar. Syst. 69, 17–28.

Kolker, A.S., Allison, M.A., Hameed, S., 2011. An evaluation of subsidence rates and sea-level variability in the Northern Gulf of Mexico. Geophys. Res. Lett. 38 (21), L21404, http://dx.doi.org/10.1029/2011GL049458.

Kolker, A.S., Kirwan, M., Goodbred, S.L., Cochran, J.K., 2010. Global climate changes recorded in coastal wetland sediments: Empirical Observations linked to theoretical predictions. Geophys. Res. Lett. 37 (14), L14706, http://dx.doi.org/10.1029/2010GL043874.

Kolker, A.S., Miner, M.D., Weathers, H.D., 2012. Depositional dynamics in a river diversion receiving basin: the case of the West Bay Mississippi River Diversion. Estuar. Coast. Shelf Sci. 106, 1–12.

Krest, J.M., Moore, W.S., Rama, 1999. ^{226}Ra and ^{228}Ra in the mixing zones of the Mississippi and Atchafalaya Rivers: indicators of groundwater input. Mar. Chem. 64, 129–152.

Kroeger, K.D., Charette, M.A., 2007. Nitrogen biogeochemistry of submarine groundwater discharge. Limnol. Oceanogr. 53 (3), 1025–1039.

LACPRA, 2012. Louisiana's Comprehensive Master Plan for a Sustainable Coast. In: Authority, L.C.P.a.R. (Ed.), Batn Rouge, pp. 170.

Lane, R.R. et al., 2007. The effects of rivrine discharge on temperature, salinity, suspended sediment and chlorophyll a in a Mississippi delta estuary measured using a flow-through system. Estuar. Coast. Shelf Sci. 74 (2007), 145–154.

LeBlanc, L.R., Mayer, L., Rufino, M., Schock, S.G., King, J., 1992. Marine sediment classification using the chirp sonar. J. Acoust. Soc. Am. 91 (1), 107–115.

Lowers, H.A. et al., 2007. Arsenic incorporation into authigenic pyrite, Bengal Basin sediment, Bangladesh. Geochim. Cosmochim. Acta 71, 2699–2717.

Martens, C.S., Kipphut, G.W., Klump, J.V., 1980. Sediment-water chemical exchange in the coastal zone traced by in situ Radon-222 flux measurements. Science 208 (441), 285–288.

Martin, J., Cable, J., Smith, C., Roy, M., Cherrier, J., 2007. Magnitudes of submarine groundwater discharge from marine and terrestrial sources: Indian River Lagoon, Florida. Water Resour. Res., W05440.

McCoy, C.A., Corbett, D.R., McKee, B.A., Top, Z., 2007. An evaluation of submarine groundwater discharge along the continental shelf of Louisiana using a multiple tracer approach. J. Geophys. Res., 112.

McCorquodale, J.A., Georgiou, I., Retana, A.G., Roblin, R.J., 2008. Assessment of integrated hydrodynamic and transport for long-term predictions, Final report submitted to CLEAR, BatonRouge, Louisiana. New Orleans, Louisiana: University of NewOrleans, Volumes I and 2, 384 pp.

McKee, B.A., Aller, R.C., Allison, M.A., Bianchi, T.S., Kineke, G.C., 2004. Transport and transformation of dissolved and particulate materials on continental margins influenced by major rivers: benthic boundary layer and seabed processes. Cont. Shelf Res. 24, 899–926.

Meade, R.H., 1996. River-sediment inputs to major deltas. In: Milliman, J.D., Haq, B. (Eds.), Sea-level Rise and Coastal Subsidence. Kluwer Academic Publishing, London, pp. 63–85.

Meade, R.H., Moody, J.A., 2010. Causes for the decline of suspended-sediment discharge in the Mississippi River system, 1940–2007. Hydrol. Process. 24, 35–49.

Meybeck, M., 1982. Carbon, nitrogen and phosphorus transport by world rivers. Am. J. Sci. 282 (4), 401–450.

Michael, H.A., Charette, M.A., Harvey, C.F., 2011. Patterns and variability of groundwater flow and radium activity at the coast: a case study from Waquoit Bay, Massachusetts. Mar. Chem. 127, 100–114.

Michael, H.A., Voss, C.I., 2009. Controls on groundwater flow in the Bengal Basin of India and Bangladesh: regional modeling analysis. Hydrogeol. J. 17 (7), 1561–1577.

Michalopoulos, P., Aller, R.C., 1995. Rapid clay mineral formation in Amazon delta sediments: reverse weathering and oceanic elemental cycles. Science 270, 614–617.

Milliman, Meade, R.H., 1983. World-wide delivery of sediment to the oceans. J. Geol. 91, 1–21.

Milliman, J.D., 1991. Flux and fate of fluvial sediment and water in coastal seas. In: Mantora, R.F.C., Martin, J.-M., Wollast, R. (Eds.), Ocean Margin Processes in Global Change. Wiley, Berlin, pp. 69–98.

Mitsch, W.J., Hernandez, M.E., 2013. Landscape and climate change threats to wetlands of North and Central America. Aquat. Sci. 75 (1), 133–149.

Moore, W.S., 1999. The subterranean estuary: a reaction zone of ground water and sea water. Mar. Chem. 65 (1–2), 111–125.

Moore, W.S., 2010. The effect of submarine groundwater discharge on the ocean. Ann. Rev. Mar. Sci. 2, 59–88.

Moore, W.S., Krest, J.M., 2004. Distribution of ^{222}Ra and ^{226}Ra in the plumes of the Mississippi and Atchafalaya River and the Gulf of Mexico. Mar. Chem. 86, 105–119.

Mulligan, A.E., Evans, R.L., Lizarralde, D., 2007. The role of paleochannels in groundwater/seawater exchange. J. Hydrol., 335.

Nelson, S.A., LeClair, S.F., 2006. Katrina's unique splay deposits in a New Orleans neighborhood. GSA Today 16 (9), 4–10.

Peng, T.H., Takahashi, T., Broecker, W.S., 1974. Surface radon measurements in the North Pacific Ocean station PAPA. J. Geophys. Res. 79, 1772–1780.

Peterson, R.N. et al., 2008. Radon and radium isotope assessment of submarine groundwater discharge in the Yellow River Delta, China. J. Geophys. Res. – Oceans 113 (C09021). http://dx.doi.org/10.1029/2008JC004776.

Prakken, L.B., Wright, L.S., 2009. Groundwater Withdrawals and Trends in Ground-Water Levels and Stream Discharge in Louisiana, US Geological Survey, In Cooperation with the Lousiana Department of Transportation and Development, Baton Rouge.

Rabalais, N.N., Turner, R.E., Wiseman, W.J., 2002. Gulf of Mexico hypoxia, aka "The dead zone". Annu. Rev. Ecol. Syst. 33, 235–263.
Rama, Moore, W.S., 1996. Using the Radium Quartet for Evaluating Groundwater exchange input and water exchange in salt marshes. Geochem. Cosmochem. Acta 60 (23), 4645–4652.
Rao, S.V.N., Bhallamudi, S.M., Thandaveswara, B.S., Sreenivasulu, V., 2005. Planning groundwater development in coastal deltas with paleo channels. Water Resour. Manage 19 (625–639).
Reed, D.J., 1995. The response of coastal marshes to sea-level rise: survival or submergence? Earth Surf. Proc. Land. 20, 39–48.
Reed, D.J. et al., 1995. Status and Trends of Hydrologic Modification, Reduction in Sediment Availability, and Habitat Loss/Modification in the Barataria-Terrebonne Estuarine System. Barataria-Terrebonne National Estuary Program, Thibodaux, LA.
Roberts, H.H., 1997. Dynamic changes of the holocene Mississippi River delta plain: the delta cycle. J. Coastal Res. 13 (3), 605–627.
Rogers, J.D. et al., 2008. Geological conditions underlying the 2005 17th Street canal levee failure in New Orleans. J. Geotech. Geoenviron. Eng. 134 (5), 583–601.
Rona, E., 1917. Diffusiongrosse und Atomdurchmesser der Radiumemanation. Zeitschrift fur Physikalische Chemie 92, 213–218.
Rouxel, O., Sholkovitz, E., Charette, M.A., Edwards, K.J., 2008. Iron isotope fractionation in subterranean estuaries. Geochim. Cosmochim. Acta 72 (14), 3413–3430.
Roy, M., Martin, J.B., Cherrier, J., Cable, J.E., Smith, C.G., 2010. Influence of sea level rise on iron diagenesis in an east Florida subterranean estuary. Geochim. Cosmochim. Acta 74 (19), 5560–5573.
Roy, M., Martin, J.B., Smith, C.G., Cable, J.E., 2011. Reactive transport modeling of iron diagenesis and associated organic carbon remineralization in a Florida (USA) subterranean estuary. Earth Planet. Sci. Lett. 304, 191–201.
Santos, I.R., Burnett, W.C., Chanton, J., Dimova, N., Peterson, R.N., 2009. Land or ocean? Assessing the driving forces of submarine groundwater discharge at a coastal site in the Gulf of Mexico. J. Geophys. Res. – Oceans 114, C04012.
Sklar, F.H., Browder, J.A., 1998. Coastal environmental impacts brought about by alterations to freshwater flow in the Gulf of Mexico. Environ. Manage. 22 (4), 547–562.
Snedden, G., Cable, J., Wiseman, W., 2007. Subtidal sea level variabiltiy in a shallow Mississippi River Deltaic Estuary, Louisiana. Estuaries Coasts 30 (5), 802–812.
Solis, R.S., Powell, G.L., 1999. Hydrography, mixing characteristics, and residence times of Gulf of Mexico estuaries. In: Bianchi, T.S., Pennock, J.R., Twilley, R.R. (Eds.), Biogeochemistry of Gulf of Mexico Estuaries. Wiley, New York, pp. 29–61.
Swarzenski, P.W. et al., 2006. Combined time-series resistivity and geochemical tracer techniques to examine submarine groundwater discharge at Dor Beach. Israel Geophys. Res. Lett. 33, L24405.
Syvitski, J.P.M., Saito, Y., 2007. Morphodynamics of deltas under the influence of humans. Global Planet. Change 57, 261–282.
Syvitski, J.P.M., Kettner, A.J., Correggiari, A., Nelson, B.W., 2005. Distributary channels and their impact on sediment dispersal. Mar. Geol. 222-223, 75–94.
Taniguchi, M., Burnett, W.C., Cable, J.E., Turner, J.V., 2002. Investigation of submarine groundwater discharge. Hydrol. Process. 16 (11), 2115–2129.
Taniguchi, M. et al., 2008. Submarine groundwater discharge from the Yellow River Delta to the Bohai Sea, China. J. Geophys. Res. 113, C06025.
Thompson, C., Smith, L., Maji, R., 2007. Hydrogeological modeling of submarine groundwater discharge on the continental shelf of Louisiana. J. Geophys. Res. 112, C03014.
Törnqvist, T.E. et al., 1996. A revised chronology for Mississippi river subdeltas. Science 273 (5282), 1693–1696.
Turner, R.E., Rabalais, N.N., Justic, D., 2006. Predicting summer hypoxia in the northern Gulf of Mexico: Riverine, N, P, and Si loading. Mar. Pollut. Bull. 52 (2), 139–148.
Valiela, I., Teal, J.M., 1979. The nitrogen budget of a salt marsh ecosystem. Nature 280, 652–656.
Vaux, H., 2011. Groundwater under stress: the importance of management. Environ. Earth Sci. 62 (1), 19–23.
Walker, J.H., 1998. Artic Deltas. J. Coastal Res. 14 (3), 718–738.
Wanninkhof, R., Mulholland, P.J., Elwood, J.W., 1990. Gas-exchange rates for a 1st-order stream determined wiht deliberate and natural tracers. Water Resour. Res. 26 (7), 1621–1630.
Weinman, B. et al., 2008. Contributions of floodplain stratigraphy and evolution to the spatial patterns of groundwater arsenic in Araihazar, Bangladesh. Geol. Soc. Am. Bull. 120 (11–12), 1567–1580.
Welder, F.A., 1955. Deltaic Processes in Cubits Gap Area, Plaquamines Parish, Louisiana, Louisiana State University, Baton Rouge, 119 pp.
Wells, J.T., Coleman, J.M., 1987. Wetland loss and the subdelta life cycle. Estuar. Coast. Shelf Sci. 25 (1), 111–125.
Werner, A.D. et al., 2013. Seawater intrusion processes, investigation and management: recent advances and future challenges. Adv. Water Resour. 51, 3–26.
Windom, H.L., Moore, W.S., Niencheski, L., Jahrike, R.A., 2006. Submarine groundwater discharge: a large, previously unrecognized source of dissolved iron to the South Atlantic Ocean. Mar. Chem. 102 (3–4), 252–266.
Yun, S.Y., Tornqvist, T.E., Hu, P., 2012. Quantifying Holocene lithospheric subsidence rates underneath the Mississippi Delta. Earth Planet. Sci. Lett. 331–332, 21–30.
Zekster, I.S., Loaiciga, H.A., 1993. Groundwater fluxes in the global hydrologic cycle: past, present, and future. J. Hydrol. 144, 405–427.